An efficient algorithm for simulating ensembles of parameterized flow problems

MAX GUNZBURGER

Department of Scientific Computing, Florida State University, Tallahassee, FL 32306-4120, USA
mgunzburger@fsu.edu

NAN JIANG

Department of Mathematics and Statistics, Missouri University of Science and Technology, Rolla, MO 65409-0020, USA
jiangn@mst.edu

AND

ZHU WANG*

Department of Mathematics, University of South Carolina, Columbia, SC 29208, USA
*Corresponding author: wangzhu@math.sc.edu

Many applications of computational fluid dynamics require multiple simulations of a flow under different input conditions. In this paper, a numerical algorithm is developed to efficiently determine a set of such simulations in which the individually independent members of the set are subject to different viscosity coefficients, initial conditions and/or body forces. The proposed scheme, when applied to the flow ensemble, needs to solve a single linear system with multiple right-hand sides, and thus is computationally more efficient than solving for all the simulations separately. We show that the scheme is nonlinearly and long-term stable under certain conditions on the time-step size and a parameter deviation ratio. A rigorous numerical error estimate shows the scheme is of first-order accuracy in time and optimally accurate in space. Several numerical experiments are presented to illustrate the theoretical results.

Keywords: Navier–Stokes equations; ensemble simulations; ensemble method.

1. Introduction

Numerical simulations of incompressible viscous flows have important applications in engineering and science. In this paper we consider settings in which one wishes to obtain solutions for several different values of the physical parameters and several different choices for the forcing functions appearing in the partial differential equation (PDE) model. For example, in building low-dimensional surrogates for the PDE solution such as sparse-grid interpolants or proper orthogonal decomposition approximations, one has to first determine expensive approximation of solutions corresponding to several values of the parameters. Sensitivity analyses of solutions often need to determine approximate solutions for several parameter values and/or forcing functions. An important third example is quantifying the uncertainties of outputs from the model equations. Mathematical models should take into account the uncertainties invariably present in the specification of physical parameters and/or forcing functions appearing in the model equations. For flow problems, because the viscosity of the liquid or gas often depends on the

temperature, an inaccurate measurement of the temperature would introduce some uncertainty into the viscosity of the flow. Direct measurements of the viscosity using flow meters and measurements of the state of the system are also prone to uncertainties. Of course, forcing functions, e.g., initial condition data, can and usually are also subject to uncertainty. In such cases, due to the lack of exact information, stochastic modeling is used to describe flows subject to a random viscosity coefficient and/or random forcing. Subsequently, numerical methods are employed to quantify the uncertainties in system output. It is known that uncertainty quantification, when a random sampling method such as a Monte Carlo method is used, could be computationally expensive for large-scale problems because each individual realization requires a large-scale computation but on the other hand, many realizations may be needed in order to obtain accurate statistical information about the outputs of interest. Therefore, for all the examples discussed and for many others, how to design efficient algorithms for performing multiple numerical simulations becomes a matter of great interest.

The ensemble method that forms the basis for our approach was proposed in Jiang & Layton (2014); there, a set of J solutions of the Navier–Stokes equations (NSE) with distinct initial conditions and forcing terms is considered. All solutions are found, at each time step, by solving a linear system with one shared coefficient matrix and J right-hand sides (RHS), reducing both the storage requirements and computational costs of the solution process. The algorithm of Jiang & Layton (2014) is first-order accurate in time; it is extended to higher-order accurate schemes in Jiang (2015, 2017). Ensemble regularization methods are developed in the studies by Jiang (2015), Jiang & Layton (2015) and Takhirov *et al.* (2016) for high Reynolds number flows, and a turbulence model based on ensemble averaging is developed in Jiang *et al.* (2015). The ensemble algorithm has also been extended to magnetohydrodynamics flows in Mohebujjaman & Rebholz (2017), to natural convection problems in Fiordilino (2017a) and to parametrized flow problems in Gunzburger *et al.* (2017b). Ensemble algorithms incorporating reduced-order modeling techniques are studied in Gunzburger *et al.* (2017a, 2018). Recently, the ensemble method has been introduced in Fiordilino (2017b); Luo & Wang (2018a,b) for uncertainty quantification problems on random linear parabolic equations.

In this paper, we develop a numerical scheme for simulating ensembles of the NSE flow problems in which not only the initial data and body force function, but also the viscosity coefficient, may vary from one ensemble member to another. Specifically, we consider a set of J NSE simulations on a bounded domain subject to no-slip boundary conditions in which the jth individual member solves the system

$$\begin{cases} u_{j,t} + u_j \cdot \nabla u_j - \nabla \cdot (\nu_j \nabla u_j) + \nabla p_j = f_j(x,t) & \text{in } \Omega \times [0,\infty), \\ \nabla \cdot u_j = 0 & \text{in } \Omega \times [0,\infty), \\ u_j = 0 & \text{on } \partial\Omega \times [0,\infty), \\ u_j(x,0) = u_j^0(x) & \text{in } \Omega, \end{cases} \tag{1.1}$$

which, for each j, corresponds to a different variable kinematic viscosity $\nu_j = \nu_j(x)$ and/or distinct initial data u_j^0 and/or body forces f_j. In the sequel, it is assumed that $\nu_j(x) \in L^\infty(\Omega)$ and $\nu_j(x) \geqslant \nu_{j,\min} > 0$.

Due to the nonlinear convection term, implicit and semiimplicit schemes are invariably used for time integration. For a semiimplicit scheme the associated discrete linear systems would be different for each individually independent simulation, i.e., for each j. As a result, at each time step, J linear systems need to be solved to determine the ensemble, resulting in a huge computational effort. For a fully implicit scheme, the situation is even worse because one would have to solve many more linear systems due to the nonlinear solver iteration. To tackle this issue we propose a novel discretization scheme that results, at each time step, in a common coefficient matrix for all the ensemble members.

1.1 *The ensemble-based semiimplicit scheme*

To focus on the main idea we temporarily ignore the spatial discretization and consider only the ensemble-based implicit–explicit temporal integration scheme

$$
\begin{cases}
\dfrac{u_j^{n+1} - u_j^n}{\Delta t} + \overline{u}^n \cdot \nabla u_j^{n+1} + (u_j^n - \overline{u}^n) \cdot \nabla u_j^n - \nabla \cdot (\overline{\nu} \nabla u_j^{n+1}) - \nabla \cdot \left((\nu_j - \overline{\nu}) \nabla u_j^n\right) + \nabla p_j^{n+1} = f_j^{n+1}, \\
\nabla \cdot u_j^{n+1} = 0,
\end{cases}
$$

(1.2)

where $\overline{u}^n$ and $\overline{\nu}$ are the ensemble means of the velocity and viscosity coefficients, respectively, defined as

$$
\overline{u}^n := \frac{1}{J} \sum_{j=1}^J u_j^n \qquad \text{and} \qquad \overline{\nu} := \frac{1}{J} \sum_{j=1}^J \nu_j.
$$

We also define $\overline{\nu}_{\min} := \frac{1}{J} \sum_{j=1}^J \nu_{j,\min}$. After rearranging the system, we have, at time t_{n+1},

$$
\begin{cases}
\dfrac{1}{\Delta t} u_j^{n+1} + \overline{u}^n \cdot \nabla u_j^{n+1} - \nabla \cdot (\overline{\nu} \nabla u_j^{n+1}) + \nabla p_j^{n+1} = f_j^{n+1} + \dfrac{1}{\Delta t} u_j^n - (u_j^n - \overline{u}^n) \cdot \nabla u_j^n + \nabla \cdot \left((\nu_j - \overline{\nu}) \nabla u_j^n\right), \\
\nabla \cdot u_j^{n+1} = 0.
\end{cases}
$$

(1.3)

It is clear that the coefficient matrix of the resulting linear system will be independent of j. Thus, for the flow ensemble, to advance all members of the ensemble by one time step, we need to solve only a single linear system with J RHS. Compared with solving J individually independent simulations, this approach used with either a single LU factorization for small-scale problems or a block Krylov subspace method (Gutknecht, 2007; Parks *et al.*, 2016) for large-scale problems is computationally more efficient and significantly reduces the required storage. When the size of the ensemble becomes huge, it can be subdivided into p sub-ensembles so as to balance memory, communication and computational costs and then (1.2) can be applied to each sub-ensemble.

The rest of this section is devoted to establishing notation and to providing other preliminary information. Then in Section 2 we prove a conditional stability result for a fully discrete finite element discretization of (1.2). In Section 3 we derive an error estimate for the fully discrete approximation. Results of the preliminary numerical simulations that illustrate the theoretical results are given in Section 4, and Section 5 provides some concluding remarks.

1.2 *Notation and preliminaries*

Let Ω denote an open, regular domain in $\mathbb{R}^d$ for $d = 2$ or 3 having boundary denoted by $\partial\Omega$. The $L^2(\Omega)$ norm and inner product are denoted by $\| \cdot \|$ and $(\cdot, \cdot)$, respectively. The $L^p(\Omega)$ norms and the Sobolev $W_p^k(\Omega)$ norms are denoted by $\| \cdot \|_{L^p}$ and $\| \cdot \|_{W_p^k}$, respectively. The Sobolev space $W_2^k(\Omega)$ is simply denoted by $H^k(\Omega)$ and its norm by $\| \cdot \|_k$. For functions $v(x, t)$ defined on $(0, T)$, we define, for $1 \leqslant m < \infty$,

$$
\|v\|_{\infty,k} := \operatorname{EssSup}_{[0,T]} \|v(\cdot, t)\|_k \qquad \text{and} \qquad \|v\|_{m,k} := \left(\int_0^T \|v(\cdot, t)\|_k^m \, \mathrm{d}t\right)^{1/m}.
$$

Given a time step Δt, associated discrete norms are defined as

$$\|v\|_{\infty,k} = \max_{0 \leqslant n \leqslant N} \|v^n\|_k \qquad \text{and} \qquad \|v\|_{m,k} := \left(\sum_{n=0}^{N} \|v^n\|_k^m \Delta t \right)^{1/m},$$

where $v^n = v(t_n)$ and $t_n = n\Delta t$. Denote by $H^{-1}(\Omega)$ the dual space of bounded linear functions on $H_0^1(\Omega) = \{v \in H^1 : v = 0 \text{ on } \partial\Omega\}$; a norm on $H^{-1}(\Omega)$ is given by

$$\|f\|_{-1} = \sup_{0 \neq v \in H_0^1(\Omega)} \frac{(f,v)}{\|\nabla v\|}.$$

The velocity space X and pressure space Q are given by

$$X := [H_0^1(\Omega)]^d \qquad \text{and} \qquad Q := L_0^2(\Omega) = \{q \in L^2(\Omega) : \int_\Omega q \, \mathrm{d}x = 0\},$$

respectively. The space of weakly divergence-free functions is

$$V := \{v \in X : (\nabla \cdot v, q) = 0, \quad \forall q \in Q\}.$$

A weak formulation of (1.1) reads as follows: for $j = 1, \ldots, J$, find $u_j : [0,T] \to X$ and $p_j : [0,T] \to Q$ for a.e. $t \in (0,T]$ satisfying

$$\begin{cases} (u_{j,t}, v) + (u_j \cdot \nabla u_j, v) + (v_j \nabla u_j, \nabla v) - (p_j, \nabla \cdot v) = (f_j, v) & \forall v \in X, \\ (\nabla \cdot u_j, q) = 0 & \forall q \in Q, \end{cases}$$

with $u_j(x,0) = u_j^0(x)$.

Our analysis is based on a finite element method (FEM) for spatial discretization. However, the results also extend, without much difficulty, to other variational discretization methods. Let $X_h \subset X$ and $Q_h \subset Q$ denote families of conforming velocity and pressure finite element spaces on a regular subdivision of Ω into simplices; the family is parameterized by the maximum diameter h of any of the simplices. Assume that the pair of spaces (X_h, Q_h) satisfy the discrete inf-sup (or LBB$_h$) condition required for the stability of the finite element approximation and that the finite element spaces satisfy the approximation properties

$$\inf_{v_h \in X_h} \|v - v_h\| \leqslant Ch^{k+1} \|u\|_{k+1} \qquad \forall v \in [H^{k+1}(\Omega)]^d, \tag{1.4}$$

$$\inf_{v_h \in X_h} \|\nabla(v - v_h)\| \leqslant Ch^k \|v\|_{k+1} \qquad \forall v \in [H^{k+1}(\Omega)]^d, \tag{1.5}$$

$$\inf_{q_h \in Q_h} \|q - q_h\| \leqslant Ch^{s+1} \|p\|_{s+1} \qquad \forall q \in H^{s+1}(\Omega), \tag{1.6}$$

where the generic constant $C > 0$ is independent of mesh size h. An example for which the LBB$_h$ stability condition and the approximation properties are satisfied is the family of Taylor–Hood P^{s+1}–P^s, $s \geqslant 1$ element pairs. For details concerning FEMs see, e.g., Ciarlet (2002) and Girault & Raviart (1979, 1986); Gunzburger (1989); Layton (2008) for FEMs for the NSE.

The discretely divergence-free subspace of X_h is defined as

$$V_h := \{v_h \in X_h : (\nabla \cdot v_h, q_h) = 0 \quad \forall q_h \in Q_h\}.$$

Note that, in general, $V_h \not\subset V$. We assume the mesh and finite element spaces satisfy the standard inverse inequality

$$h\|\nabla v_h\| \leqslant C_{(\text{inv})}\|v_h\| \quad \forall v_h \in X_h, \tag{1.7}$$

which is known to hold for standard finite element spaces with locally quasi-uniform meshes (Brenner & Scott, 2008). We also define the standard explicitly skew-symmetric trilinear form

$$b^*(u, v, w) := \tfrac{1}{2}(u \cdot \nabla v, w) - \tfrac{1}{2}(u \cdot \nabla w, v),$$

which satisfies the bounds (Layton, 2008)

$$b^*(u, v, w) \leqslant C \left(\|\nabla u\| \|u\|\right)^{1/2} \|\nabla v\| \|\nabla w\| \quad \forall u, v, w \in X, \tag{1.8}$$

$$b^*(u, v, w) \leqslant C\|\nabla u\| \|\nabla v\| \left(\|\nabla w\| \|w\|\right)^{1/2} \quad \forall u, v, w \in X. \tag{1.9}$$

We also denote the exact and approximate solutions at $t = t^n$ as u_j^n and $u_{j,h}^n$, respectively.

2. Stability analysis

The fully discrete finite element discretization of (1.2) is given as follows. Given $u_{j,h}^0 \in X_h$, for $n = 0, 1, \ldots, N - 1$, find $u_{j,h}^{n+1} \in X_h$ and $p_{j,h}^{n+1} \in Q_h$ satisfying

$$
\begin{cases}
\left(\dfrac{u_{j,h}^{n+1} - u_{j,h}^n}{\Delta t}, v_h\right) + b^*(\overline{u}_h^n, u_{j,h}^{n+1}, v_h) + b^*(u_{j,h}^n - \overline{u}_h^n, u_{j,h}^n, v_h) - (p_{j,h}^{n+1}, \nabla \cdot v_h) \\
\qquad + (\overline{\nu}\nabla u_{j,h}^{n+1}, \nabla v_h) + \left((\nu_j - \overline{\nu})\nabla u_{j,h}^n, \nabla v_h\right) = (f_j^{n+1}, v_h) \quad \forall v_h \in X_h, \\
\left(\nabla \cdot u_{j,h}^{n+1}, q_h\right) = 0 \quad \forall q_h \in Q_h.
\end{cases}
\tag{2.1}
$$

We begin by proving the conditional, nonlinear, long-time stability of scheme (2.1) under a time-step condition and a parameter deviation condition.

THEOREM 2.1 (Stability). For all $j = 1, \ldots, J$, if for some $\mu, 0 \leqslant \mu < 1$, and some $\varepsilon, 0 < \varepsilon \leqslant 2 - 2\sqrt{\mu}$, the following time-step condition and parameter deviation condition both hold,

$$C\frac{\Delta t}{h\overline{\nu}_{\min}} \left\|\nabla(u_{j,h}^n - \overline{u}_h^n)\right\|^2 \leqslant \frac{(2 - 2\sqrt{\mu} - \varepsilon)\sqrt{\mu}}{2(\sqrt{\mu} + \varepsilon)}, \tag{2.2}$$

$$\frac{\|\nu_j - \overline{\nu}\|_\infty}{\overline{\nu}_{\min}} \leqslant \sqrt{\mu}, \tag{2.3}$$

then scheme (2.1) is nonlinearly, long-time stable. In particular, for $j = 1, \ldots, J$ and for any $N \geqslant 1$, we have

$$
\begin{aligned}
&\frac{1}{2}\|u_{j,h}^N\|^2 + \frac{1}{4}\sum_{n=0}^{N-1}\|u_{j,h}^{n+1} - u_{j,h}^n\|^2 + \sum_{n=0}^{N-1}\frac{\varepsilon(2-\sqrt{\mu})}{4(\sqrt{\mu}+\varepsilon)}\overline{v}_{\min}\Delta t\|\nabla u_{j,h}^{n+1}\|^2 \\
&\quad + \overline{v}_{\min}\Delta t\left(\frac{\sqrt{\mu}}{2}\frac{2+\varepsilon}{\sqrt{\mu}+\varepsilon} - \frac{\|v_j - \overline{v}\|_\infty}{2\overline{v}_{\min}}\right)\|\nabla u_{j,h}^N\|^2 \qquad (2.4) \\
&\leqslant \sum_{n=0}^{N-1}\frac{2\Delta t}{\overline{v}_{\min}}\|f_j^{n+1}\|_{-1}^2 + \frac{1}{2}\|u_{j,h}^0\|^2 + \overline{v}_{\min}\Delta t\left(\frac{\sqrt{\mu}}{2}\frac{2+\varepsilon}{\sqrt{\mu}+\varepsilon} - \frac{\|v_j - \overline{v}\|_\infty}{2\overline{v}_{\min}}\right)\|\nabla u_{j,h}^0\|^2.
\end{aligned}
$$

Proof. The proof is given in Appendix A. $\qquad\square$

REMARK 2.2 It is seen from (2.2) that the upper bound in the time-step condition increases as ε decreases. As $\varepsilon \to 0$ the bound approaches $1 - \sqrt{\mu}$. Because the relative deviation of the viscosity coefficient in (2.3) is bounded by $\sqrt{\mu}$, the two stability conditions are oppositional to each other.

REMARK 2.3 Noting that condition (2.2) depends only on known quantities such as the solution at t_n and that scheme (2.1) is a one-step method, (2.2) can be used to adapt Δt in order to guarantee stability for the ensemble simulations.

REMARK 2.4 When the viscosity v_j is a constant instead of being variable, the relative viscosity coefficient deviation ratio required for stability is still bounded by $\sqrt{\mu}$, and condition (2.3) becomes $\max_j \frac{|v_j - \overline{v}|}{\overline{v}} \leqslant \sqrt{\mu}$.

3. Error analysis

In this section we give a detailed error analysis of the proposed method under the same type of time-step condition (with possibly a different constant C on the left-hand side of the inequality) and the same parameter deviation condition. Assuming that X_h and Q_h satisfy the LBB_h condition, scheme (2.1) is equivalent to the following: given $u_{j,h}^0 \in V_h$, for $n = 0, 1, \ldots, N-1$ find $u_{j,h}^{n+1} \in V_h$ such that

$$
\begin{aligned}
&\left(\frac{u_{j,h}^{n+1} - u_{j,h}^n}{\Delta t}, v_h\right) + b^*(\overline{u}_h^n, u_{j,h}^{n+1}, v_h) + b^*(u_{j,h}^n - \overline{u}_h^n, u_{j,h}^n, v_h) \\
&\quad + \overline{v}(\nabla u_{j,h}^{n+1}, \nabla v_h) + ((v_j - \overline{v})\nabla u_{j,h}^n, \nabla v_h) = (f_j^{n+1}, v_h) \quad \forall v_h \in V_h. \qquad (3.1)
\end{aligned}
$$

To analyse the rate of convergence of the approximation we assume the following regularity for the exact solutions:

$$
u_j \in L^\infty(0, T; H^{k+1}(\Omega)) \cap H^1(0, T; H^{k+1}(\Omega)) \cap H^2(0, T; L^2(\Omega)),
$$

$$
p_j \in L^2(0, T; H^{s+1}(\Omega)) \quad \text{and} \quad f_j \in L^2(0, T; L^2(\Omega)).
$$

Let $e_j^n = u_j^n - u_{j,h}^n$ denote the approximation error of the jth simulation at the time instance t_n. We then have the following error estimates.

THEOREM 3.1 (Convergence of scheme (2.1)). For all $j = 1, \ldots, J$, if for some $\mu, 0 \leqslant \mu < 1$ and some $\varepsilon, 0 < \varepsilon \leqslant 2 - 2\sqrt{\mu}$ the following time-step condition and parameter deviation condition both hold,

$$C\frac{\Delta t}{\overline{v}_{\min}h}\left\| \nabla(u_{j,h}^n - \overline{u}_h^n)\right\|^2 \leqslant \frac{(2 - 2\sqrt{\mu} - \varepsilon)\sqrt{\mu}}{2(\sqrt{\mu} + \varepsilon)}, \tag{3.2}$$

$$\frac{\|v_j - \overline{v}\|_\infty}{\overline{v}_{\min}} \leqslant \sqrt{\mu}, \tag{3.3}$$

then there exists a positive constant C independent of the time step such that

$$\frac{1}{2}\|e_j^N\|^2 + \frac{1}{15}\frac{\varepsilon}{\sqrt{\mu} + \varepsilon}\left(1 - \frac{\sqrt{\mu}}{2}\right)\overline{v}_{\min}\Delta t \sum_{n=0}^{N-1}\|\nabla e_j^{n+1}\|^2$$

$$\leqslant e^{\frac{CT}{\overline{v}_{\min}^3}}\left\{ \frac{1}{2}\|e_j^0\|^2 + \left(\frac{\sqrt{\mu}}{2}\frac{(2+\varepsilon)}{\sqrt{\mu}+\varepsilon} - \frac{\|v_j - \overline{v}\|_\infty}{2\overline{v}_{\min}}\right)\overline{v}_{\min}\Delta t\|\nabla e_j^0\|^2 \right.$$

$$+ \frac{1}{2}h^{2k+2}\|u_j^0\|_{k+1}^2 + \left(\frac{\sqrt{\mu}}{2}\frac{(2+\varepsilon)}{\sqrt{\mu}+\varepsilon} - \frac{\|v_j - \overline{v}\|_\infty}{2\overline{v}_{\min}}\right)\overline{v}_{\min}\Delta t h^{2k}\|u_j^0\|_{k+1}^2$$

$$+ C\Delta t^2\frac{\|v_j - \overline{v}\|_\infty^2}{\overline{v}_{\min}}\|\nabla u_{j,t}\|_{2,0}^2 + C\overline{v}_{\min}h^{2k}\|u_j\|_{2,k+1}^2 + C\frac{\|v_j - \overline{v}\|_\infty^2}{\overline{v}_{\min}}h^{2k}\|u_j\|_{2,k+1}^2$$

$$+ Ch^{2k+1}\Delta t^{-1}\|u_j\|_{2,k+1}^2 + Ch\Delta t\|\nabla u_{j,t}\|_{2,0}^2 + C\overline{v}_{\min}^{-1}h^{2k}\|u_j\|_{2,k+1}^2$$

$$+ C\overline{v}_{\min}^{-1}\Delta t^2\|\nabla u_{j,t}\|_{2,0}^2 + C\overline{v}_{\min}^{-1}h^{2k}\|u_j\|_{4,k+1}^4 + C\overline{v}_{\min}^{-1}h^{2k}$$

$$+ C\overline{v}_{\min}^{-1}h^{2s+2}\|p_j\|_{2,s+1}^2 + C\overline{v}_{\min}^{-1}h^{2k+2}\|u_{j,t}\|_{2,k+1}^2 + C\overline{v}_{\min}^{-1}\Delta t^2\|u_{j,tt}\|_{2,0}^2 \right\}$$

$$+ \frac{1}{2}h^{2k+2}\|u_j\|_{\infty,k+1}^2 + \frac{1}{15}\frac{\varepsilon}{\sqrt{\mu}+\varepsilon}\left(1 - \frac{\sqrt{\mu}}{2}\right)\overline{v}_{\min}h^{2k}\|u_j\|_{2,k+1}^2.$$

Proof. The proof is given in Appendix B. □

In particular, when Taylor–Hood elements ($k = 2$, $s = 1$) are used, i.e., the C^0 piecewise-quadratic velocity space X_h and the C^0 piecewise-linear pressure space Q_h, we have the following estimate.

COROLLARY 3.2 Assume that $\|e_j^0\|$ and $\|\nabla e_j^0\|$ are both $\mathscr{O}(h)$ accurate or better. Then if (X_h, Q_h) is chosen as the (P_2, P_1) Taylor–Hood element pair, we have

$$\frac{1}{2}\|e_j^N\|^2 + \frac{1}{15}\frac{\varepsilon}{\sqrt{\mu}+\varepsilon}\left(1 - \frac{\sqrt{\mu}}{2}\right)\overline{v}_{\min}\Delta t \sum_{n=0}^{N-1}\|\nabla e_j^{n+1}\|^2 \leqslant C(h^2 + \Delta t^2 + h\Delta t).$$

4. Numerical experiments

In this section we illustrate the effectiveness of our proposed method (1.2) and the associated theoretical analyses in Sections 2 and 3 by considering two examples: a Green–Taylor vortex problem and a flow between two offset cylinders. The first problem has a known exact solution that is used to illustrate the error analysis. The second example does not have an analytic solution but has complex flow structures; it is used to check the stability analysis and demonstrate the necessity and efficiency of the proposed method.

4.1   *The Green–Taylor vortex problem*

The Green–Taylor vortex flow is commonly used for testing convergence rates, e.g., see Chorin (1968), Tafti (1996), John & Layton (2002), Berselli (2005), Barbato *et al.* (2007) and Jiang & Tran (2015). The Green–Taylor vortex solution given by

$$u(x, y, t) = -\cos(\omega\pi x)\sin(\omega\pi y)e^{-2\omega^2\pi^2 t/\tau},$$
$$v(x, y, t) = \sin(\omega\pi x)\cos(\omega\pi y)e^{-2\omega^2\pi^2 t/\tau}, \tag{4.1}$$
$$p(x, y, t) = -\tfrac{1}{4}(\cos(2\omega\pi x) + \cos(2\omega\pi y))e^{-4\omega^2\pi^2 t/\tau}$$

satisfies the NSE in $\Omega = (0, 1)^2$ for $\tau = \mathrm{Re}$ and initial condition

$$u^0 = \left(-\cos(\omega\pi x)\sin(\omega\pi y), \sin(\omega\pi x)\cos(\omega\pi y)\right)^{\mathrm{T}}.$$

The solution consists of an $\omega \times \omega$ array of oppositely signed vortices that decay as $t \to \infty$. In the following numerical tests we take $\omega = 1$, $\nu = 1/\mathrm{Re}$, $T = 1$, $h = 1/m$ and $\Delta t/h = 2/5$. The boundary condition is assumed to be inhomogeneous Dirichlet, that is, the boundary values match that of the exact solution.

We consider an ensemble of two members, u_1 and u_2, corresponding to two incompressible NSE simulations with different viscosity coefficients ν_j and initial conditions $u_{j,0}$. We investigate the ensemble simulations and compare them with independent simulations. For $j = 1, 2$ we define by $\mathscr{E}_j^E = u_j - u_{j,h}$ the approximation error of the jth member of the ensemble simulation and by $\mathscr{E}_j^S = u_j - u_{j,h}$ the approximation error of the jth independently determined simulation. Here, the superscript '*E*' stands for 'ensemble' whereas '*S*' stands for 'independent'.
Case 1. We set the viscosity coefficient $\nu_1 = 0.2$ and initial condition $u_{1,0} = (1 + \varepsilon)u^0$ for the first member u_1 and $\nu_2 = 0.3$ and $u_{2,0} = (1 - \varepsilon)u^0$ for the second member u_2, where $\varepsilon = 10^{-3}$. For this choice of parameters, we have $|\nu_j - \overline{\nu}|/\overline{\nu} = \frac{1}{5}$ for both $j = 1$ and $j = 2$ so that condition (2.3) is satisfied. We first apply the ensemble algorithm; results are shown in Table 1. It is seen that the convergence rate for u_1 and u_2 is first order.

We next compare the ensemble simulations with independent simulations. To this end, we perform each NSE simulation independently using the same discretization setup. The associated approximation errors are listed in Table 2. Comparing with Table 1, we observe that the ensemble simulation is able to achieve accuracies close to those of the independent, more costly simulations.

TABLE 1 *For the Green–Taylor vortex problem (Case 1) and for a sequence of uniform grid sizes h, errors for ensemble simulations of two members with inputs $v_1 = 0.2$, $u_{1,0} = (1+10^{-3})u^0$ and $v_2 = 0.3$, $u_{2,0} = (1 - 10^{-3})u^0$*

$1/h$	$\|\mathscr{E}_1^E\|_{\infty,0}$	Rate	$\|\nabla\mathscr{E}_1^E\|_{2,0}$	Rate	$\|\mathscr{E}_2^E\|_{\infty,0}$	Rate	$\|\nabla\mathscr{E}_2^E\|_{2,0}$	Rate
20	$1.05 \cdot 10^{-2}$	–	$4.17 \cdot 10^{-2}$	–	$7.36 \cdot 10^{-3}$	–	$2.53 \cdot 10^{-2}$	–
40	$5.86 \cdot 10^{-3}$	0.85	$2.21 \cdot 10^{-2}$	0.91	$3.87 \cdot 10^{-3}$	0.93	$1.31 \cdot 10^{-2}$	0.95
80	$3.10 \cdot 10^{-3}$	0.92	$1.14 \cdot 10^{-2}$	0.95	$2.02 \cdot 10^{-3}$	0.94	$6.70 \cdot 10^{-3}$	0.97
160	$1.59 \cdot 10^{-3}$	0.96	$5.81 \cdot 10^{-3}$	0.97	$1.03 \cdot 10^{-3}$	0.97	$3.39 \cdot 10^{-3}$	0.98

TABLE 2 *For the Green–Taylor vortex problem (Case 1) and for a sequence of uniform grid sizes h, errors in independent simulations of two members with inputs $v_1 = 0.2$, $u_{1,0} = (1 + 10^{-3})u^0$ and $v_2 = 0.3$, $u_{2,0} = (1 - 10^{-3})u^0$*

$1/h$	$\|\mathscr{E}_1^S\|_{\infty,0}$	Rate	$\|\nabla\mathscr{E}_1^S\|_{2,0}$	Rate	$\|\mathscr{E}_2^S\|_{\infty,0}$	Rate	$\|\nabla\mathscr{E}_2^S\|_{2,0}$	Rate
20	$1.01 \cdot 10^{-2}$	–	$3.88 \cdot 10^{-2}$	–	$7.88 \cdot 10^{-3}$	–	$2.76 \cdot 10^{-2}$	–
40	$5.47 \cdot 10^{-3}$	0.89	$2.04 \cdot 10^{-2}$	0.93	$4.24 \cdot 10^{-3}$	0.90	$1.44 \cdot 10^{-2}$	0.93
80	$2.85 \cdot 10^{-3}$	0.94	$1.05 \cdot 10^{-2}$	0.96	$2.22 \cdot 10^{-3}$	0.93	$7.41 \cdot 10^{-3}$	0.96
160	$1.46 \cdot 10^{-3}$	0.97	$5.30 \cdot 10^{-3}$	0.98	$1.13 \cdot 10^{-3}$	0.97	$3.76 \cdot 10^{-3}$	0.98

TABLE 3 *For the Green–Taylor vortex problem (Case 2) and for a sequence of uniform grid sizes h, errors in ensemble simulations of two members: $v_1 = 0.01$, $u_{1,0} = (1 + 10^{-3})u^0$ and $v_2 = 0.49$, $u_{2,0} = (1 - 10^{-3})u^0$*

$1/h$	$\|\mathscr{E}_1^E\|_{\infty,0}$	Rate	$\|\nabla\mathscr{E}_1^E\|_{2,0}$	Rate	$\|\mathscr{E}_2^E\|_{\infty,0}$	Rate	$\|\nabla\mathscr{E}_2^E\|_{2,0}$	Rate
20	$2.91 \cdot 10^{-2}$	–	$2.96 \cdot 10^{-1}$	–	$3.50 \cdot 10^{-3}$	–	$9.94 \cdot 10^{-3}$	–
40	$1.86 \cdot 10^{-2}$	0.65	$1.80 \cdot 10^{-1}$	0.71	$1.65 \cdot 10^{-3}$	1.08	$4.97 \cdot 10^{-3}$	1
80	$1.08 \cdot 10^{-2}$	0.78	$1.02 \cdot 10^{-1}$	0.83	$8.53 \cdot 10^{-4}$	0.95	$2.52 \cdot 10^{-3}$	0.98
160	$5.89 \cdot 10^{-3}$	0.87	$5.46 \cdot 10^{-2}$	0.90	$4.32 \cdot 10^{-4}$	0.98	$1.27 \cdot 10^{-3}$	0.98

Case 2. We now set $v_1 = 0.01$ and $v_2 = 0.49$ while keeping the same initial conditions as for Case 1. With this choice of parameters, $|v_j - \overline{v}|/\overline{v} = \frac{24}{25}$ for both $j = 1$ and $j = 2$, which still satisfies (2.3) but is closer to the upper limit. The ensemble simulation errors are listed in Table 3, which shows that the rate of convergence for the second member is nearly 1 and for the first member is approaching 1.

The approximation errors for two independent simulations under the same discretization setup are listed in Table 4. Comparing the ensemble simulation results in Table 3 with the independent simulations, we find that the accuracy of the first member in the ensemble simulation degrades slightly whereas that of the second member in the ensemble simulation improves a bit. Overall, the ensemble simulation is able to achieve the same order of accuracy as the independent simulations.

4.2 *Flow between two offset cylinders*

Next we check the stability of our algorithm by considering the problem of a flow between two offset circles (see, e.g., Jiang & Layton, 2014, 2015; Jiang, 2015; Jiang *et al.*, 2015). The domain is a disk with

TABLE 4   *For the Green–Taylor vortex problem (Case 2) and for a sequence of uniform grid sizes h,
errors in independent simulations of two members:* $\nu_1 = 0.01$, $u_{1,0} = (1 + 10^{-3})u^0$ *and* $\nu_2 = 0.49$,
$u_{2,0} = (1 - 10^{-3})u^0$

$1/h$	$\|\mathcal{E}_1^S\|_{\infty,0}$	Rate	$\|\nabla\mathcal{E}_1^S\|_{2,0}$	Rate	$\|\mathcal{E}_2^S\|_{\infty,0}$	Rate	$\|\nabla\mathcal{E}_2^S\|_{2,0}$	Rate
20	$3.19 \cdot 10^{-2}$	–	$2.95 \cdot 10^{-1}$	–	$5.49 \cdot 10^{-3}$	–	$1.79 \cdot 10^{-2}$	–
40	$1.67 \cdot 10^{-2}$	0.93	$1.54 \cdot 10^{-1}$	0.93	$3.03 \cdot 10^{-3}$	0.86	$9.38 \cdot 10^{-3}$	0.94
80	$8.56 \cdot 10^{-3}$	0.97	$7.90 \cdot 10^{-2}$	0.97	$1.59 \cdot 10^{-3}$	0.93	$4.81 \cdot 10^{-3}$	0.96
160	$4.33 \cdot 10^{-3}$	0.98	$3.99 \cdot 10^{-2}$	0.98	$8.18 \cdot 10^{-4}$	0.96	$2.44 \cdot 10^{-3}$	0.98

a smaller off-center obstacle inside. Letting $r_1 = 1$, $r_2 = 0.1$ and $c = (c_1, c_2) = \left(\frac{1}{2}, 0\right)$, the domain is
given by

$$\Omega = \left\{(x, y) \ : \ x^2 + y^2 \leqslant r_1^2 \text{ and } (x - c_1)^2 + (y - c_2)^2 \geqslant r_2^2\right\}.$$

The flow is driven by a counterclockwise rotational body force

$$f(x, y, t) = \left(-6y(1 - x^2 - y^2), 6x(1 - x^2 - y^2)\right)^{\mathrm{T}}$$

with no-slip boundary conditions imposed on both circles. The flow between the two circles shows
interesting structures interacting with the inner circle. A von Kármán vortex street is formed behind
the inner circle and then re-interacts with that circle and with itself, generating complex flow patterns.
We consider multiple numerical simulations of the flow with different viscosity coefficients using the
ensemble-based algorithm (2.1). For spatial discretization, we apply the Taylor–Hood element pair on a
triangular mesh that is generated by Delaunay triangulation with 80 mesh points on the outer circle and
60 mesh points on the inner circle and with refinement near the inner circle, resulting in 18,638 degrees
of freedom; see Fig. 1.

   In order to illustrate the stability analysis, we select two different sets of viscosity coefficients for

Case 1: $\nu_1 = 0.005$, $\nu_2 = 0.039$, $\nu_3 = 0.016$;

Case 2: $\nu_1 = 0.005$, $\nu_2 = 0.041$, $\nu_3 = 0.014$.

Note that the viscosity coefficients in Case 2 are obtained by slightly perturbing those in Case 1. The
average of the viscosity coefficients is $\bar{\nu} = 0.02$ for both cases. However, the stability condition (2.3) is
satisfied in the first case but is not satisfied in the second one, i.e., we have

Case 1: $\frac{|\nu_1 - \bar{\nu}|}{\bar{\nu}} = \frac{3}{4} < 1$, $\frac{|\nu_2 - \bar{\nu}|}{\bar{\nu}} = \frac{19}{20} < 1$, $\frac{|\nu_3 - \bar{\nu}|}{\bar{\nu}} = \frac{1}{5} < 1$;

Case 2: $\frac{|\nu_1 - \bar{\nu}|}{\bar{\nu}} = \frac{3}{4} < 1$, $\frac{|\nu_2 - \bar{\nu}|}{\bar{\nu}} = \frac{21}{20} > 1$, $\frac{|\nu_3 - \bar{\nu}|}{\bar{\nu}} = \frac{3}{10} < 1$.

The second member of Case 2 has a perturbation ratio greater than 1. Simulations of both cases are
subject to the same initial condition and body forces for all ensemble members. In particular, the initial
condition is generated by solving the steady Stokes problem with viscosity $\nu = 0.02$ and the same
body force $f(x, y, t)$. All the simulations are run over the time interval $[0, 5]$ with a time-step size
$\Delta t = 0.01$. This time-step size is smaller than the one ensuring a stable ensemble simulation in Case 1,
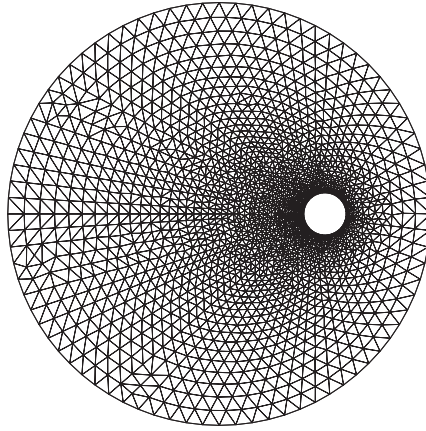
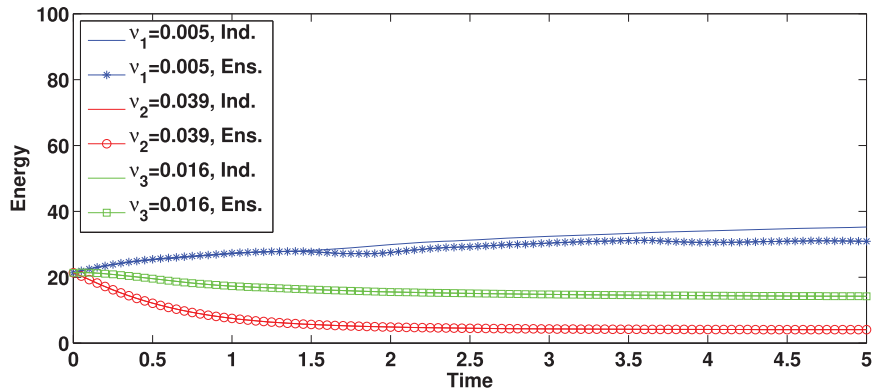FIG. 1. Mesh for the flow between two offset cylinders example.

FIG. 2. For the flow between two offset cylinders, Case 1, the energy evolution of the ensemble (Ens.) and independent simulations (Ind.).

thus condition (2.2) holds. Furthermore, the same Δt is used in Case 2. Because the viscosity coefficients in Case 2 are slightly perturbed from those in Case 1, and Δt is chosen small, we believe condition (2.2) still holds. But condition (2.3) no longer holds. Therefore, we expect the ensemble simulation to be unstable even when using the small time-step size $\Delta t = 0.01$. For testing the stability, we use the kinetic energy as a criterion and compare the ensemble simulation results with independent simulations using the same mesh and time-step size.

The comparison of the energy evolution of ensemble-based simulations with the corresponding independent simulations is shown in Figs 2 and 3. It is seen that for Case 1 the ensemble simulation is stable, but for Case 2 it becomes unstable. This phenomenon coincides with our stability analysis since condition (2.3) holds for all members of Case 1, but does not hold for the second member of Case 2. Indeed, it is observed from Fig. 3 that the energy of the second member in Case 2 blows up after $t = 3.7$, then affecting the other two members, and this results in their energy dramatically increasing after $t = 4.7$.
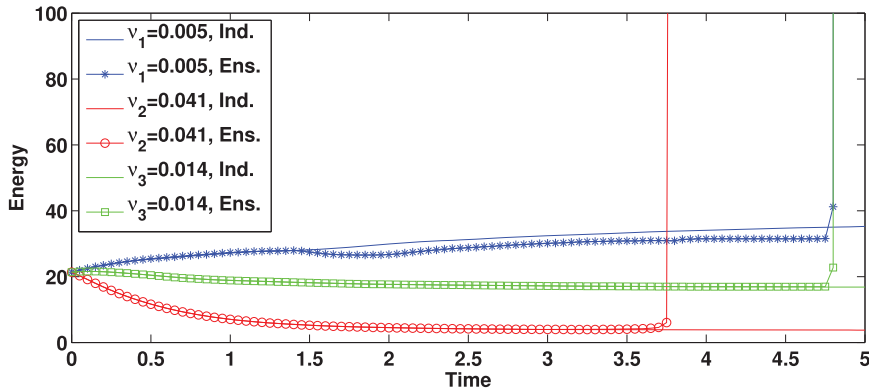
FIG. 3. For the flow between two offset cylinders, Case 2, the energy evolution of the ensemble (Ens.) and independent simulations (Ind.).

Next we use this test example to illustrate the necessity of ensemble simulations. Indeed, the ensemble calculation is much needed when flow problems are under parameter uncertainty. This is because even though one could obtain a 'best estimate' of the parameter that is close enough to the true parameter value, the corresponding individual solution may vary significantly from the true solution due to the nonlinearity of the problems. However, the ensemble mean of the model problems at several selected parameter samples, which are drawn from a probability distribution (usually experimentally determined), tends to smooth out possible errors and gives a better forecast than the single run using the 'best estimate' parameter value. Here we consider a simple computational setting in which the true viscosity $\nu = 0.01$. Due to the errors in measurements, the 'best estimate' of the viscosity is 0.00995. Suppose the viscosity value empirically follows a uniform distribution on [0.009, 0.011]. We first run the simulation with viscosity $\nu = 0.01$ on the domain partitioned by a Delaunay triangular mesh with 80 mesh points on the outer circle and 40 mesh points on the inner circle, take the uniform time-step size to be $\Delta t = 0.002$ and label the output solution 'true' as it is the numerical solution associated with the true datum.

We then run the simulation associated to the 'best estimate' $\nu = 0.00995$ and label its solution 'best estimate', which is to be compared with the ensemble forecast. For the latter, we draw J (= 16, 32, 64) independent, uniformly distributed samples of ν from [0.009, 0.011], and seek the mean of these J simulation results by using the proposed ensemble algorithm. Time evolution of the kinetic energy for the single 'best estimate' ensemble means of J simulations are shown in Fig. 4, together with that of the 'true' solution. It is observed that although the 'best estimate' of ν is very close to the true value, the difference between these two solutions is relatively large. However, the ensemble mean is able to yield a more accurate forecast. The greater the number of realizations, the better forecast that ensemble mean could achieve.

Finally, we illustrate the efficiency of the proposed ensemble algorithm. To this end, we solve a group of J flow problems using a sequence of individual simulations and one ensemble simulation, respectively. These problems are subject to fixed initial and boundary conditions and a forcing function, but different viscosity parameter values. We then compare the efficiency of these two approaches by considering the CPU time. Assume the viscosity parameter ν_j to be a random variable that distributes uniformly on the interval [0.4, 0.5]. We generate a set of J (= 2, 4, 8, 16) random samples using MATLAB, partition the domain by a Delaunay triangular mesh with 80 mesh points on the outer circle
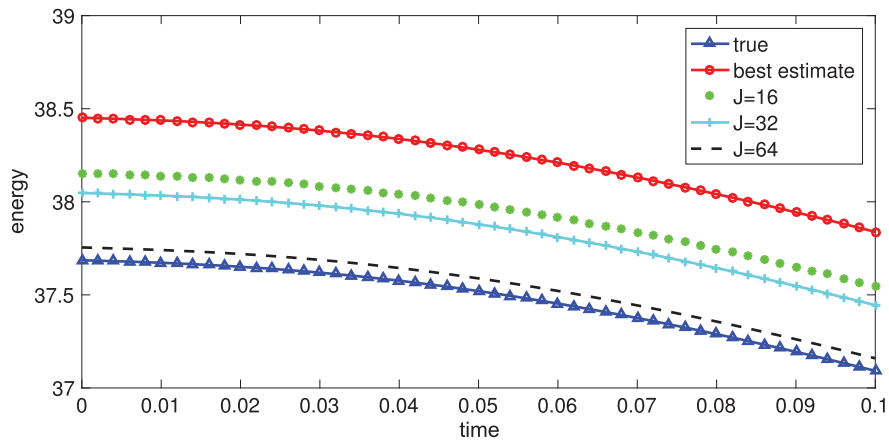
FIG. 4. For the flow between two offset cylinders, comparison of 'true' solution, 'best estimate' solution and ensemble forecast.

TABLE 5 *Efficiency comparison between the ensemble simulations and individual simulations on a set of J parametrized NSE flow between two offset cylinders problems at $T = 0.1$. It is observed that the ensemble algorithm outperforms the individual simulations as the former spends less CPU times than the latter but keeps the same accuracy*

J	$\|\bar{u}^E(T)\|$	CPU (s)	$\|\bar{u}^S(T)\|$	CPU (s)
2	1.9870	44.2404	1.9870	101.244
4	1.8674	60.9567	1.8674	199.142
8	1.8893	95.1164	1.8893	397.261
16	1.9227	164.637	1.9227	788.407

and 40 mesh points on the inner circle and take the uniform time-step size to be $\Delta t = 0.002$. Both individual and ensemble simulations are implemented by using FreeFem++ with UMFPACK, which solves the linear system with multifrontal LU factorization. Numerical results together with the CPU time for simulations (measured in seconds) are listed in Table 5, where $\|\bar{u}^E(T)\|$ is the L_2 norm of the mean of the velocity obtained by the ensemble algorithm (2.1) at the final simulation time $T = 0.1$ and $\|\bar{u}^S(T)\|$ is that of individual simulations.

Define the speedup factor of the ensemble algorithm to be the ratio of execution time for the sequence of individual simulations to that of the ensemble simulation. It is observed that for this simple test, the computational time for completing the sequence of individual simulations increases almost linearly as the size of the ensemble increases, which is expected as all the work including assembly of matrices and LU decomposition needs to be done repeatedly for each ensemble member. However, the ensemble algorithm takes significantly less CPU time while maintaining the same accuracy. It is seen that for $J = 2$ the speedup factor is 2.30, while for $J = 16$ the speedup factor increases to 4.81. This saving rate will keep increasing as the size of the ensemble increases.

5. Conclusions

In this paper, we consider a set of Navier–Stokes simulations in which each member may be subject to a distinct viscosity coefficient, initial conditions and/or body forces. An ensemble algorithm is developed for the group by which all the flow ensemble members, after discretization, share a common linear system with different right-hand-side vectors. This leads to a great saving in both storage requirements and computational costs. The stability and accuracy of the ensemble method are analysed. Two numerical experiments are presented. The first is for Green–Taylor flow and serves to illustrate the first-order accuracy in time of the ensemble-based scheme. The second is for a flow between two offset cylinders and serves to show that our stability analysis is sharp and the proposed method is effective. As a next step, we will investigate higher-order accurate schemes for the flow ensemble simulations.

Funding

References

Barbato, D., Berselli, L. & Grisanti, C. (2007) Analytical and numerical results for the rational large eddy simulation model. *J. Math. Fluid Mech.*, **9**, 44–74.

Berselli, L. (2005) On the large eddy simulation of the Taylor-Green vortex. *J. Math. Fluid Mech.*, **7**, S164–S191.

Brenner, S. & Scott, R. (2008) *The Mathematical Theory of Finite Element Methods*, 3rd edn. New York: Springer-Verlag

Chorin, A. (1968) Numerical solution for the Navier–Stokes equations. *Math. Comp.*, **22**, 745–762.

Ciarlet, P. (2002) *The Finite Element Method for Elliptic Problems*. Philadelphia: SIAM.

Fiordilino, J. (2017a) A second order ensemble timestepping algorithm for natural convection. Preprint, arXiv:1708.00488.

Fiordilino, J. (2017b) Ensemble timestepping algorithms for the heat equation with uncertain conductivity. Preprint, arXiv:1708.00893.

Girault, V. & Raviart, P.-A. (1979) *Finite Element Approximation of the Navier-Stokes Equations*. Lecture Notes in Mathematics, vol. 749. Berlin: Springer.

Girault, V. & Raviart, P.-A. (1986) *Finite Element Methods for Navier-Stokes Equations - Theory and Algorithms*. Berlin: Springer.

Gunzburger, M. (1989) *Finite Element Methods for Viscous Incompressible Flows - A Guide to Theory, Practice, and Algorithms*. London: Academic Press.

Gunzburger, M., Jiang, N. & Schneier, M. (2017a) An ensemble-proper orthogonal decomposition method for the nonstationary Navier-Stokes equations. *SIAM J. Numer. Anal.*, **55**, 286–304.

Gunzburger, M., Jiang, N. & Schneier, M. (2018) A higher-order ensemble/proper orthogonal decomposition method for the nonstationary Navier-Stokes equations. *Int. J. Numer. Anal. Model.*, **15**, 608–627.

Gunzburger, M., Jiang, N. & Wang, Z. (2017b) A second-order time-stepping scheme for simulating ensembles of parameterized flow problems. *Comput. Meth. Appl. Math.* (in press). https://doi.org/10.1515/cmam-2017-0051.

Gutknecht, M. (2007) Block Krylov space methods for linear systems with multiple right-hand sides: an introduction. *Modern Mathematical Models, Methods and Algorithms for Real World Systems* (A. H. Siddiqi, I. S. Duff and O. Christensen eds). New Delhi: Anamaya Publishers, pp. 420–447.

Jiang, N. (2015) A higher order ensemble simulation algorithm for fluid flows. *J. Sci. Comput.*, **64**, 264–288.

Jiang, N. (2017) A second-order ensemble method based on a blended backward differentiation formula timestepping scheme for time-dependent Navier-Stokes equations. *Numer. Meth. Partial. Diff. Eqs.*, **33**, 34–61.

JIANG, N. & LAYTON, W. (2014) An algorithm for fast calculation of flow ensembles. *Int. J. Uncertain. Quantif.*, **4**, 273–301.

JIANG, N. & LAYTON, W. (2015) Numerical analysis of two ensemble eddy viscosity numerical regularizations of fluid motion. *Numer. Meth. Partial Diff. Eqs.*, **31**, 630–651.

JIANG, N. & TRAN, H. (2015) Analysis of a stabilized CNLF method with fast slow wave splittings for flow problems. *Comput. Meth. Appl. Math.*, **15**, 307–330.

JIANG, N., KAYA, S. & LAYTON, W. (2015) Analysis of model variance for ensemble based turbulence modeling. *Comput. Meth. Appl. Math.*, **15**, 173–188.

JOHN, V. & LAYTON, W. (2002) Analysis of numerical errors in large eddy simulation. *SIAM J. Numer. Anal.*, **40**, 995–1020.

LAYTON, W. (2008) *Introduction to the Numerical Analysis of Incompressible Viscous Flows*. Philadelphia: Society for Industrial and Applied Mathematics (SIAM).

LUO, Y. & WANG, Z. (2018a) An ensemble algorithm for numerical solutions to deterministic and random parabolic PDEs. *SIAM J. Numer. Anal.*, **56**, 859–876.

LUO, Y. & WANG, Z. (2018b) A multilevel Monte Carlo ensemble scheme for solving random parabolic PDEs. Preprint, arXiv:1802.05743.

MOHEBUJJAMAN, M. & REBHOLZ, L. (2017) An efficient algorithm for computation of MHD flow ensembles. *Comput. Meth. Appl. Math.*, **17**, 121–138.

PARKS, M., SOODHALTER, K. M. & SZYLD, D. B. (2016) A block recycled GMRES method with investigations into aspects of solver performance. Preprint, arXiv:1604.01713.

TAFTI, D. (1996) Comparison of some upwind-biased high-order formulations with a second order central-difference scheme for time integration of the incompressible Navier-Stokes equations. *Comput. & Fluids*, **25**, 647–665.

TAKHIROV, A., NEDA, M. & WATERS, J. (2016) Time relaxation algorithm for flow ensembles. *Numer. Meth. Partial Diff. Eqs.*, **32**, 757–777.

THOMÉE, V. (1997) *Galerkin Finite Element Methods for Parabolic Problems*. Berlin, Heidelberg: Springer.

Appendix A. Proof of Theorem 2.1

Setting $v_h = u_{j,h}^{n+1}$ and $q_h = p_{j,h}^{n+1}$ in (2.1) and then adding two equations we obtain

$$\frac{1}{2}\|u_{j,h}^{n+1}\|^2 - \frac{1}{2}\|u_{j,h}^n\|^2 + \frac{1}{2}\|u_{j,h}^{n+1} - u_{j,h}^n\|^2 + \Delta t b^*(u_{j,h}^n - \overline{u}_h^n, u_{j,h}^n, u_{j,h}^{n+1})$$
$$+ \Delta t \|\overline{v}^{\frac{1}{2}} \nabla u_{j,h}^{n+1}\|^2 = \Delta t(f_j^{n+1}, u_{j,h}^{n+1}) - \Delta t\left((v_j - \overline{v})\nabla u_{j,h}^n, \nabla u_{j,h}^{n+1}\right).$$

Note that $\overline{v} \geqslant \overline{v}_{\min} > 0$. We apply Young's inequality to the terms on the RHS and have, for all $\alpha, \beta > 0$,

$$\frac{1}{2}\|u_{j,h}^{n+1}\|^2 - \frac{1}{2}\|u_{j,h}^n\|^2 + \frac{1}{2}\|u_{j,h}^{n+1} - u_{j,h}^n\|^2 + \overline{v}_{\min}\Delta t\|\nabla u_{j,h}^{n+1}\|^2 + \Delta t b^*\left(u_{j,h}^n - \overline{u}_h^n, u_{j,h}^n, u_{j,h}^{n+1} - u_{j,h}^n\right)$$
$$\leqslant \frac{\alpha \overline{v}_{\min}\Delta t}{8}\|\nabla u_{j,h}^{n+1}\|^2 + \frac{2\Delta t}{\alpha \overline{v}_{\min}}\|f_j^{n+1}\|_{-1}^2 + \frac{\beta \overline{v}_{\min}\Delta t}{4}\|\nabla u_{j,h}^{n+1}\|^2 + \frac{\|v_j - \overline{v}\|_\infty^2 \Delta t}{\beta \overline{v}_{\min}}\|\nabla u_{j,h}^n\|^2. \tag{A1}$$

Both $\frac{\beta \overline{v}_{\min}\Delta t}{4}\|\nabla u_{j,h}^{n+1}\|^2$ and $\frac{\|v_j-\overline{v}\|_\infty^2 \Delta t}{\beta \overline{v}_{\min}}\|\nabla u_{j,h}^n\|^2$ on the RHS of (A1) need to be absorbed into $\overline{v}_{\min}\Delta t\|\nabla u_{j,h}^{n+1}\|^2$ on the LHS. To this end, we minimize $\frac{\beta \overline{v}_{\min}\Delta t}{4} + \frac{\|v_j-\overline{v}\|_\infty^2 \Delta t}{\beta \overline{v}_{\min}}$ by selecting $\beta = \frac{2\|v_j-\overline{v}\|_\infty}{\overline{v}_{\min}}$

so that (A1) becomes

$$\frac{1}{2}\|u_{j,h}^{n+1}\|^2 - \frac{1}{2}\|u_{j,h}^n\|^2 + \frac{1}{2}\|u_{j,h}^{n+1} - u_{j,h}^n\|^2 + \overline{v}_{\min}\Delta t\|\nabla u_{j,h}^{n+1}\|^2 + \Delta t b^*(u_{j,h}^n - \overline{u}_h^n, u_{j,h}^n, u_{j,h}^{n+1} - u_{j,h}^n)$$

$$\leqslant \frac{\alpha\overline{v}_{\min}\Delta t}{8}\|\nabla u_{j,h}^{n+1}\|^2 + \frac{2\Delta t}{\alpha\overline{v}_{\min}}\|f_j^{n+1}\|_{-1}^2 + \frac{\|v_j - \overline{v}\|_\infty\Delta t}{2}\|\nabla u_{j,h}^{n+1}\|^2 + \frac{\|v_j - \overline{v}\|_\infty\Delta t}{2}\|\nabla u_{j,h}^n\|^2. \tag{A2}$$

Next we bound the trilinear term using the inequality (1.9) and the inverse inequality (1.7), obtaining

$$-\Delta t b^*(u_{j,h}^n - \overline{u}_h^n, u_{j,h}^n, u_{j,h}^{n+1} - u_{j,h}^n) \leqslant C\Delta t\|\nabla(u_{j,h}^n - \overline{u}_h^n)\|\|\nabla u_{j,h}^n\|\left[\|\nabla(u_{j,h}^{n+1} - u_{j,h}^n)\|\|u_{j,h}^{n+1} - u_{j,h}^n\|\right]^{1/2}$$

$$\leqslant C\Delta t\|\nabla(u_{j,h}^n - \overline{u}_h^n)\|\|\nabla u_{j,h}^n\|Ch^{-\frac{1}{2}}\|u_{j,h}^{n+1} - u_{j,h}^n\|.$$

Using Young's inequality again gives

$$-\Delta t b^*(u_{j,h}^n - \overline{u}_h^n, u_{j,h}^n, u_{j,h}^{n+1} - u_{j,h}^n) \leqslant C\frac{\Delta t^2}{h}\|\nabla(u_{j,h}^n - \overline{u}_h^n)\|^2\|\nabla u_{j,h}^n\|^2 + \frac{1}{4}\|u_{j,h}^{n+1} - u_{j,h}^n\|^2. \tag{A3}$$

Substituting (A3) into (A2) and combining like terms, we have

$$\frac{1}{2}\|u_{j,h}^{n+1}\|^2 - \frac{1}{2}\|u_{j,h}^n\|^2 + \frac{1}{4}\|u_{j,h}^{n+1} - u_{j,h}^n\|^2 + \overline{v}_{\min}\Delta t\left(1 - \frac{\alpha}{4} - \frac{\|v_j - \overline{v}\|_\infty}{2\overline{v}_{\min}}\right)\|\nabla u_{j,h}^{n+1}\|^2$$

$$+ \frac{\alpha}{8}\overline{v}_{\min}\Delta t\|\nabla u_{j,h}^{n+1}\|^2 \leqslant \frac{2\Delta t}{\alpha\overline{v}_{\min}}\|f_j^{n+1}\|_{-1}^2 + C\frac{\Delta t^2}{h}\|\nabla(u_{j,h}^n - \overline{u}_h^n)\|^2\|\nabla u_{j,h}^n\|^2$$

$$+ \frac{\|v_j - \overline{v}\|_\infty\Delta t}{2}\|\nabla u_{j,h}^n\|^2.$$

For any $0 < \sigma < 1$,

$$\frac{1}{2}\|u_{j,h}^{n+1}\|^2 - \frac{1}{2}\|u_{j,h}^n\|^2 + \frac{1}{4}\|u_{j,h}^{n+1} - u_{j,h}^n\|^2 + \frac{\alpha}{8}\overline{v}_{\min}\Delta t\|\nabla u_{j,h}^{n+1}\|^2$$

$$+ \overline{v}_{\min}\Delta t\left(1 - \frac{\alpha}{4} - \frac{\|v_j - \overline{v}\|_\infty}{2\overline{v}_{\min}}\right)\left(\|\nabla u_{j,h}^{n+1}\|^2 - \|\nabla u_{j,h}^n\|^2\right)$$

$$+ \overline{v}_{\min}\Delta t\left[(1 - \sigma)\left(1 - \frac{\alpha}{4} - \frac{\|v_j - \overline{v}\|_\infty}{2\overline{v}_{\min}}\right) - \frac{C\Delta t}{\overline{v}_{\min}h}\|\nabla(u_{j,h}^n - \overline{u}_h^n)\|^2\right]\|\nabla u_{j,h}^n\|^2$$

$$+ \overline{v}_{\min}\Delta t\left[\sigma\left(1 - \frac{\alpha}{4} - \frac{\|v_j - \overline{v}\|_\infty}{2\overline{v}_{\min}}\right) - \frac{\|v_j - \overline{v}\|_\infty}{2\overline{v}_{\min}}\right]\|\nabla u_{j,h}^n\|^2 \leqslant \frac{2\Delta t}{\alpha\overline{v}_{\min}}\|f_j^{n+1}\|_{-1}^2. \tag{A4}$$

Select $\alpha = 4 - \frac{2(\sigma+1)}{\sigma}\sqrt{\mu}$. Since α is supposed to be greater than 0, we have

$$\sigma > \frac{\sqrt{\mu}}{2 - \sqrt{\mu}} \in (0, 1). \tag{A5}$$

Now taking $\sigma = \frac{\sqrt{\mu}+\varepsilon}{2-\sqrt{\mu}}$, where $\varepsilon \in (0, 2 - 2\sqrt{\mu})$, (A4) becomes

$$
\begin{aligned}
&\frac{1}{2}\|u_{j,h}^{n+1}\|^2 - \frac{1}{2}\|u_{j,h}^n\|^2 + \frac{1}{4}\|u_{j,h}^{n+1} - u_{j,h}^n\|^2 + \frac{\alpha}{8}\overline{\nu}_{\min}\Delta t\|\nabla u_{j,h}^{n+1}\|^2 \\
&\quad + \overline{\nu}_{\min}\Delta t\Big(1 - \frac{\alpha}{4} - \frac{\|\nu_j - \overline{\nu}\|_\infty}{2\overline{\nu}_{\min}}\Big)\Big(\|\nabla u_{j,h}^{n+1}\|^2 - \|\nabla u_{j,h}^n\|^2\Big) \\
&\quad + \overline{\nu}_{\min}\Delta t\bigg[\Big((1-\sigma)\frac{\sigma+1}{2\sigma}\sqrt{\mu} - (1-\sigma)\frac{\|\nu_j - \overline{\nu}\|_\infty}{2\overline{\nu}_{\min}}\Big) - \frac{C\Delta t}{\overline{\nu}_{\min}h}\|\nabla(u_{j,h}^n - \overline{u}_h^n)\|^2\bigg]\|\nabla u_{j,h}^n\|^2 \\
&\quad + \overline{\nu}_{\min}\Delta t\bigg[\frac{\sigma+1}{2}\sqrt{\mu} - (1+\sigma)\frac{\|\nu_j - \overline{\nu}\|_\infty}{2\overline{\nu}_{\min}}\bigg]\|\nabla u_{j,h}^n\|^2 \leqslant \frac{2\Delta t}{\alpha\overline{\nu}_{\min}}\|f_j^{n+1}\|_{-1}^2 .
\end{aligned}
\tag{A6}
$$

Stability follows if the following conditions hold:

$$
(1-\sigma)\frac{\sigma+1}{2\sigma}\sqrt{\mu} - (1-\sigma)\frac{1}{2}\frac{\|\nu_j - \overline{\nu}\|_\infty}{\overline{\nu}_{\min}} - \frac{C\Delta t}{\overline{\nu}_{\min}h}\|\nabla(u_{j,h}^n - \overline{u}_h^n)\|^2 \geqslant 0,
\tag{A7}
$$

$$
\frac{\sigma+1}{2}\sqrt{\mu} - (1+\sigma)\frac{\|\nu_j - \overline{\nu}\|_\infty}{2\overline{\nu}_{\min}} \geqslant 0.
\tag{A8}
$$

Using assumption (2.3), we have

$$
\frac{\sigma+1}{2}\sqrt{\mu} - (1+\sigma)\frac{\|\nu_j - \overline{\nu}\|_\infty}{2\overline{\nu}_{\min}} = \frac{2+\varepsilon}{2-\sqrt{\mu}}\left(\frac{\sqrt{\mu}}{2} - \frac{\|\nu_j - \overline{\nu}\|_\infty}{2\overline{\nu}_{\min}}\right) \geqslant 0
$$

so that (A7) holds. Together with assumption (2.2), we then have

$$
\begin{aligned}
&(1-\sigma)\frac{\sigma+1}{2\sigma}\sqrt{\mu} - (1-\sigma)\frac{1}{2}\frac{\|\nu_j - \overline{\nu}\|_\infty}{\overline{\nu}_{\min}} - \frac{C\Delta t}{\overline{\nu}_{\min}h}\|\nabla(u_{j,h}^n - \overline{u}_h^n)\|^2 \\
&\quad \geqslant (1-\sigma)\frac{\sigma+1}{2\sigma}\sqrt{\mu} - (1-\sigma)\frac{1}{2}\sqrt{\mu} - \frac{C\Delta t}{\overline{\nu}_{\min}h}\|\nabla(u_{j,h}^n - \overline{u}_h^n)\|^2 \\
&\quad = \frac{(2 - 2\sqrt{\mu} - \varepsilon)\sqrt{\mu}}{2(\sqrt{\mu} + \varepsilon)} - \frac{(2 - 2\sqrt{\mu} - \varepsilon)\sqrt{\mu}}{2(\sqrt{\mu} + \varepsilon)} = 0,
\end{aligned}
$$

so (A8) holds. Therefore, assuming that (2.2) and (2.3) hold, (A6) reduces to

$$
\begin{aligned}
&\frac{1}{2}\|u_{j,h}^{n+1}\|^2 - \frac{1}{2}\|u_{j,h}^n\|^2 + \frac{1}{4}\|u_{j,h}^{n+1} - u_{j,h}^n\|^2 + \frac{\varepsilon(2 - \sqrt{\mu})}{4(\sqrt{\mu} + \varepsilon)}\overline{\nu}_{\min}\Delta t\|\nabla u_{j,h}^{n+1}\|^2 \\
&\quad + \overline{\nu}_{\min}\Delta t\left(\frac{\sqrt{\mu}}{2}\frac{2+\varepsilon}{\sqrt{\mu} + \varepsilon} - \frac{\|\nu_j - \overline{\nu}\|_\infty}{2\overline{\nu}_{\min}}\right)\Big(\|\nabla u_{j,h}^{n+1}\|^2 - \|\nabla u_{j,h}^n\|^2\Big) \leqslant \frac{2\Delta t}{\overline{\nu}_{\min}}\|f_j^{n+1}\|_{-1}^2 .
\end{aligned}
\tag{A9}
$$

Summing (A9) from $n = 0$ to $n = N - 1$ results in

$$
\begin{aligned}
\frac{1}{2}\|u_{j,h}^N\|^2 &+ \frac{1}{4}\sum_{n=0}^{N-1}\|u_{j,h}^{n+1} - u_{j,h}^n\|^2 + \sum_{n=0}^{N-1}\frac{\varepsilon(2 - \sqrt{\mu})}{4(\sqrt{\mu} + \varepsilon)}\overline{v}_{\min}\Delta t\|\nabla u_{j,h}^{n+1}\|^2 \\
&+ \overline{v}_{\min}\Delta t\left(\frac{\sqrt{\mu}}{2}\frac{2 + \varepsilon}{\sqrt{\mu} + \varepsilon} - \frac{\|v_j - \overline{v}\|_\infty}{2\overline{v}_{\min}}\right)\|\nabla u_{j,h}^N\|^2 \\
&\leqslant \sum_{n=0}^{N-1}\frac{2\Delta t}{\overline{v}_{\min}}\|f_j^{n+1}\|_{-1}^2 + \frac{1}{2}\|u_{j,h}^0\|^2 + \overline{v}_{\min}\Delta t\left(\frac{\sqrt{\mu}}{2}\frac{2 + \varepsilon}{\sqrt{\mu} + \varepsilon} - \frac{\|v_j - \overline{v}\|_\infty}{2\overline{v}_{\min}}\right)\|\nabla u_{j,h}^0\|^2. \quad \text{(A10)}
\end{aligned}
$$

This completes the proof of stability.

Appendix B. Proof of Theorem 3.1

The weak solution of the NSE u_j satisfies

$$
\begin{aligned}
\left(\frac{u_j^{n+1} - u_j^n}{\Delta t}, v_h\right) &+ b^*(u_j^{n+1}, u_j^{n+1}, v_h) + (v_j\nabla u_j^{n+1}, \nabla v_h) \\
&- (p_j^{n+1}, \nabla \cdot v_h) = (f_j^{n+1}, v_h) + \text{Intp}(u_j^{n+1}; v_h) \qquad \forall\, v_h \in V_h, \quad \text{(B1)}
\end{aligned}
$$

where $\text{Intp}(u_j^{n+1}; v_h) = \left(\frac{u_j^{n+1} - u_j^n}{\Delta t} - u_{j,t}(t^{n+1}), v_h\right)$.

Let

$$
e_j^n = u_j^n - u_{j,h}^n = (u_j^n - R_h u_j^n) + (R_h u_j^n - u_{j,h}^n) = \eta_j^n + \xi_{j,h}^n,
$$

where $R_h u_j^n \in V_h$ is the Ritz projection of u_j^n onto V_h defined by $\left(\overline{v}\ \nabla(u_j^n - R_h u_j^n), \nabla v_h\right) = 0$. The associated Ritz projection error satisfies (see, e.g., Thomée, 1997)

$$
\|R_h u_j^n - u_j^n\| + h\|\nabla(R_h u_j^n - u_j^n)\| \leqslant Ch^{k+1}\|u_j^n\|_{k+1}. \quad \text{(B2)}
$$

Subtracting (3.1) from (B1) gives

$$
\begin{aligned}
\left(\frac{\xi_{j,h}^{n+1} - \xi_{j,h}^n}{\Delta t}, v_h\right) &+ (\overline{v}\nabla\xi_{j,h}^{n+1}, \nabla v_h) + ((v_j - \overline{v})\nabla(u_j^{n+1} - u_j^n), \nabla v_h) + ((v_j - \overline{v})\nabla\xi_{j,h}^n, \nabla v_h) \\
&+ b^*(u_j^{n+1}, u_j^{n+1}, v_h) - b^*(\overline{u}_h^n, u_{j,h}^{n+1}, v_h) - b^*(u_{j,h}^n - \overline{u}_h^n, u_{j,h}^n, v_h) - (p_j^{n+1}, \nabla \cdot v_h) \\
&= -\left(\frac{\eta_j^{n+1} - \eta_j^n}{\Delta t}, v_h\right) - (\overline{v}\nabla\eta_j^{n+1}, \nabla v_h) - ((v_j - \overline{v})\nabla\eta_j^n, \nabla v_h) + \text{Intp}(u_j^{n+1}; v_h).
\end{aligned}
$$

Setting $v_h = \xi_{j,h}^{n+1} \in V_h$ and rearranging the nonlinear terms, we have

$$
\frac{1}{\Delta t}\left(\frac{1}{2}\|\xi_{j,h}^{n+1}\|^2 - \frac{1}{2}\|\xi_{j,h}^n\|^2 + \frac{1}{2}\|\xi_{j,h}^{n+1} - \xi_{j,h}^n\|^2\right) + \|\overline{\nu}^{\frac{1}{2}}\nabla\xi_{j,h}^{n+1}\|^2
$$

$$
= -((\nu_j - \overline{\nu})\nabla(u_j^{n+1} - u_j^n), \nabla\xi_{j,h}^{n+1}) - ((\nu_j - \overline{\nu})\nabla\xi_{j,h}^n, \nabla\xi_{j,h}^{n+1}) - ((\nu_j - \overline{\nu})\nabla\eta_j^n, \nabla\xi_{j,h}^{n+1})
$$

$$
- b^*(u_{j,h}^n - \overline{u}_h^n, u_{j,h}^{n+1} - u_{j,h}^n, \xi_{j,h}^{n+1}) - b^*(u_j^{n+1}, u_j^{n+1}, \xi_{j,h}^{n+1}) + b^*(u_{j,h}^n, u_{j,h}^{n+1}, \xi_{j,h}^{n+1}) \tag{B3}
$$

$$
+ (p_j^{n+1}, \nabla\cdot\xi_{j,h}^{n+1}) - \left(\frac{\eta_j^{n+1} - \eta_j^n}{\Delta t}, \xi_{j,h}^{n+1}\right) + \mathrm{Intp}(u_j^{n+1}; \xi_{j,h}^{n+1}).
$$

We first bound the viscous terms on the RHS of (B3):

$$
-((\nu_j - \overline{\nu})\nabla(u_j^{n+1} - u_j^n), \nabla\xi_{j,h}^{n+1}) \leqslant \|\nu_j - \overline{\nu}\|_\infty\|\nabla(u_j^{n+1} - u_j^n)\|\|\nabla\xi_{j,h}^{n+1}\|
$$

$$
\leqslant \frac{1}{4C_0}\frac{\|\nu_j - \overline{\nu}\|_\infty^2}{\overline{\nu}_{\min}}\|\nabla(u_j^{n+1} - u_j^n)\|^2 + C_0\overline{\nu}_{\min}\|\nabla\xi_{j,h}^{n+1}\|^2
$$

$$
\leqslant \frac{\Delta t}{4C_0}\frac{\|\nu_j - \overline{\nu}\|_\infty^2}{\overline{\nu}_{\min}}\left(\int_{t^n}^{t^{n+1}}\|\nabla u_{j,t}\|^2\,\mathrm{d}t\right) + C_0\overline{\nu}_{\min}\|\nabla\xi_{j,h}^{n+1}\|^2, \tag{B4}
$$

$$
-((\nu_j - \overline{\nu})\nabla\eta_j^n, \nabla\xi_{j,h}^{n+1}) \leqslant \|\nu_j - \overline{\nu}\|_\infty\|\nabla\eta_j^n\|\|\nabla\xi_{j,h}^{n+1}\|
$$

$$
\leqslant \frac{1}{4C_0}\frac{\|\nu_j - \overline{\nu}\|_\infty^2}{\overline{\nu}_{\min}}\|\nabla\eta_j^n\|^2 + C_0\overline{\nu}_{\min}\|\nabla\xi_{j,h}^{n+1}\|^2, \tag{B5}
$$

$$
-(\nu_j - \overline{\nu})(\nabla\xi_{j,h}^n, \nabla\xi_{j,h}^{n+1}) \leqslant \|\nu_j - \overline{\nu}\|_\infty\|\nabla\xi_{j,h}^n\|\|\nabla\xi_{j,h}^{n+1}\|
$$

$$
\leqslant \frac{1}{4C_1}\frac{\|\nu_j - \overline{\nu}\|_\infty^2}{\overline{\nu}_{\min}}\|\nabla\xi_{j,h}^n\|^2 + C_1\overline{\nu}_{\min}\|\nabla\xi_{j,h}^{n+1}\|^2
$$

$$
\leqslant \frac{\|\nu_j - \overline{\nu}\|_\infty}{2}\|\nabla\xi_{j,h}^n\|^2 + \frac{\|\nu_j - \overline{\nu}\|_\infty}{2}\|\nabla\xi_{j,h}^{n+1}\|^2, \tag{B6}
$$

in which we note that both terms on the RHS of (B6) need to be hidden in the LHS of the error equation, thus $C_1 = \frac{\|\nu_j - \overline{\nu}\|_\infty}{2\overline{\nu}_{\min}}$ is selected to minimize the summation.

Next we analyse the nonlinear terms on the RHS of (B3) one by one. For the first nonlinear term we have

$$
-b^*(u_{j,h}^n - \overline{u}_h^n, u_{j,h}^{n+1} - u_{j,h}^n, \xi_{j,h}^{n+1}) = -b^*(u_{j,h}^n - \overline{u}_h^n, e_j^{n+1} - e_j^n, \xi_{j,h}^{n+1}) + b^*(u_{j,h}^n - \overline{u}_h^n, u_j^{n+1} - u_j^n, \xi_{j,h}^{n+1})
$$

$$
= -b^*(u_{j,h}^n - \overline{u}_h^n, \eta_j^{n+1}, \xi_{j,h}^{n+1}) + b^*(u_{j,h}^n - \overline{u}_h^n, \eta_j^n, \xi_{j,h}^{n+1})
$$

$$
+ b^*(u_{j,h}^n - \overline{u}_h^n, \xi_j^n, \xi_{j,h}^{n+1}) + b^*(u_{j,h}^n - \overline{u}_h^n, u_j^{n+1} - u_j^n, \xi_{j,h}^{n+1}). \tag{B7}
$$

Using inequality (1.8) and Young's inequality, we have the estimates

$$-b^*(u_{j,h}^n - \overline{u}_h^n, \eta_j^{n+1}, \xi_{j,h}^{n+1}) \leqslant C\|\nabla(u_{j,h}^n - \overline{u}_h^n)\|\|\nabla\eta_j^{n+1}\|\|\nabla\xi_{j,h}^{n+1}\|$$

$$\leqslant \frac{C^2}{4C_0}\overline{\nu}_{\min}^{-1}\|\nabla(u_{j,h}^n - \overline{u}_h^n)\|^2\|\nabla\eta_j^{n+1}\|^2 + C_0\overline{\nu}_{\min}\|\nabla\xi_{j,h}^{n+1}\|^2 \qquad (B8)$$

and

$$-b^*(u_{j,h}^n - \overline{u}_h^n, \eta_j^n, \xi_{j,h}^{n+1}) \leqslant C\|\nabla(u_{j,h}^n - \overline{u}_h^n)\|\|\nabla\eta_j^n\|\|\nabla\xi_{j,h}^{n+1}\|$$

$$\leqslant \frac{C^2}{4C_0}\overline{\nu}_{\min}^{-1}\|\nabla(u_{j,h}^n - \overline{u}_h^n)\|^2\|\nabla\eta_j^n\|^2 + C_0\overline{\nu}_{\min}\|\nabla\xi_{j,h}^{n+1}\|^2. \qquad (B9)$$

Because $b^*(\cdot, \cdot, \cdot)$ is skew-symmetric we have

$$b^*(u_{j,h}^n - \overline{u}_h^n, \xi_{j,h}^n, \xi_{j,h}^{n+1}) = b^*(u_{j,h}^n - \overline{u}_h^n, \xi_{j,h}^n - \xi_{j,h}^{n+1}, \xi_{j,h}^{n+1})$$

$$= b^*(u_{j,h}^n - \overline{u}_h^n, \xi_{j,h}^{n+1}, \xi_{j,h}^{n+1} - \xi_{j,h}^n).$$

Then by inequality (1.8) we obtain

$$b^*(u_{j,h}^n - \overline{u}_h^n, \xi_{j,h}^n, \xi_{j,h}^{n+1}) \leqslant \|\nabla(u_{j,h}^n - \overline{u}_h^n)\|\|\nabla\xi_{j,h}^n\|\|\nabla(\xi_{j,h}^{n+1} - \xi_{j,h}^n)\|^{1/2}\|\xi_{j,h}^{n+1} - \xi_{j,h}^n\|^{1/2}$$

$$\leqslant C\|\nabla(u_{j,h}^n - \overline{u}_h^n)\|\|\nabla\xi_{j,h}^n\|h^{-1/2}\|\xi_{j,h}^{n+1} - \xi_{j,h}^n\|$$

$$\leqslant \frac{1}{4\Delta t}\|\xi_{j,h}^{n+1} - \xi_{j,h}^n\|^2 + \left[C\frac{\Delta t}{h}\|\nabla(u_{j,h}^n - \overline{u}_h^n)\|^2\right]\|\nabla\xi_{j,h}^n\|^2. \qquad (B10)$$

For the last term of (B7) we have

$$b^*(u_{j,h}^n - \overline{u}_h^n, u_j^{n+1} - u_j^n, \xi_{j,h}^{n+1}) \leqslant C\|\nabla(u_{j,h}^n - \overline{u}_h^n)\|\|\nabla(u_j^{n+1} - u_j^n)\|\|\nabla\xi_{j,h}^{n+1}\| \qquad (B11)$$

$$\leqslant \frac{C^2}{4C_0}\overline{\nu}_{\min}^{-1}\|\nabla(u_{j,h}^n - \overline{u}_h^n)\|^2\|\nabla(u_j^{n+1} - u_j^n)\|^2 + C_0\overline{\nu}_{\min}\|\nabla\xi_{j,h}^{n+1}\|^2$$

$$\leqslant \frac{C^2}{4C_0}\Delta t\overline{\nu}_{\min}^{-1}\|\nabla(u_{j,h}^n - \overline{u}_h^n)\|^2\left(\int_{t^n}^{t^{n+1}}\|\nabla u_{j,t}\|^2\,\mathrm{d}t\right) + C_0\overline{\nu}_{\min}\|\nabla\xi_{j,h}^{n+1}\|^2.$$

Next we bound the last two nonlinear terms on the RHS of (B3) as

$$-b^*(u_j^{n+1}, u_j^{n+1}, \xi_{j,h}^{n+1}) + b^*(u_{j,h}^n, u_{j,h}^n, \xi_{j,h}^{n+1})$$

$$= -b^*(e_j^n, u_j^{n+1}, \xi_{j,h}^{n+1}) - b^*(u_{j,h}^n, e_j^{n+1}, \xi_{j,h}^{n+1}) - b^*(u_j^{n+1} - u_j^n, u_j^{n+1}, \xi_{j,h}^{n+1})$$

$$= -b^*(\eta_j^n, u_j^{n+1}, \xi_{j,h}^{n+1}) - b^*(\xi_{j,h}^n, u_j^{n+1}, \xi_{j,h}^{n+1}) - b^*(u_{j,h}^n, \eta_j^{n+1}, \xi_{j,h}^{n+1}) - b^*(u_j^{n+1} - u_j^n, u_j^{n+1}, \xi_{j,h}^{n+1}),$$
$$(B12)$$

where, with the assumption $u_j^{n+1} \in L^\infty(0, T; H^1(\Omega))$, we have

$$-b^*(\eta_j^n, u_j^{n+1}, \xi_{j,h}^{n+1}) \leqslant C\|\nabla\eta_j^n\|\|\nabla u_j^{n+1}\|\|\nabla\xi_{j,h}^{n+1}\|$$

$$\leqslant \frac{C^2}{4C_0}\overline{\nu}_{\min}^{-1}\|\nabla\eta_j^n\|^2 + C_0\overline{\nu}_{\min}\|\nabla\xi_{j,h}^{n+1}\|^2. \qquad (B13)$$

Using inequality (1.8), Young's inequality and $u_j^{n+1} \in L^\infty(0, T; H^1(\Omega))$ we get

$$
\begin{aligned}
-b^*(\xi_{j,h}^n, u_j^{n+1}, \xi_{j,h}^{n+1}) &\leqslant C \|\nabla \xi_{j,h}^n\|^{1/2} \|\xi_{j,h}^n\|^{1/2} \|\nabla u_j^{n+1}\| \|\nabla \xi_{j,h}^{n+1}\| \leqslant C \|\nabla \xi_{j,h}^n\|^{1/2} \|\xi_{j,h}^n\|^{1/2} \|\nabla \xi_{j,h}^{n+1}\| \\
&\leqslant C \Big(\frac{1}{4\alpha} \|\nabla \xi_{j,h}^n\| \|\xi_{j,h}^n\| + \alpha \|\nabla \xi_{j,h}^{n+1}\|^2 \Big) \\
&\leqslant C \Big[\frac{1}{4\alpha} \Big(\frac{\Delta}{2} \|\nabla \xi_{j,h}^n\|^2 + \frac{1}{2\Delta} \|\xi_{j,h}^n\|^2 \Big) + \alpha \|\nabla \xi_{j,h}^{n+1}\|^2 \Big] \\
&\leqslant C_0 \overline{\nu}_{\min} \|\nabla \xi_{j,h}^n\|^2 + \frac{C^4}{64 C_0^3 \overline{\nu}_{\min}^3} \|\xi_{j,h}^n\|^2 + C_0 \overline{\nu}_{\min} \|\nabla \xi_{j,h}^{n+1}\|^2,
\end{aligned}
\tag{B14}
$$

where we set $\alpha = \frac{C_0 \overline{\nu}_{\min}}{C}$ and $\Delta = \frac{8 C_0^2 \overline{\nu}_{\min}^2}{C^2}$. By Young's inequality, (1.8) and the result (A10) from the stability analysis, i.e., $\|u_{j,h}^n\|^2 \leqslant C$, we also have

$$
\begin{aligned}
b^*(u_{j,h}^n, \eta_j^{n+1}, \xi_{j,h}^{n+1}) &\leqslant C \|\nabla u_{j,h}^n\|^{1/2} \|u_{j,h}^n\|^{1/2} \|\nabla \eta_j^{n+1}\| \|\nabla \xi_{j,h}^{n+1}\| \\
&\leqslant \frac{C^2}{4 C_0} \overline{\nu}_{\min}^{-1} \|\nabla u_{j,h}^n\| \|\nabla \eta_j^{n+1}\|^2 + C_0 \overline{\nu}_{\min} \|\nabla \xi_{j,h}^{n+1}\|^2
\end{aligned}
\tag{B15}
$$

and

$$
\begin{aligned}
b^*(u_j^{n+1} - u_j^n, u_j^{n+1}, \xi_{j,h}^{n+1}) &\leqslant C \|\nabla(u_j^{n+1} - u_j^n)\| \|\nabla u_j^{n+1}\| \|\nabla \xi_{j,h}^{n+1}\| \\
&\leqslant \frac{C^2}{4 C_0} \overline{\nu}_{\min}^{-1} \|\nabla(u_j^{n+1} - u_j^n)\|^2 + C_0 \overline{\nu}_{\min} \|\nabla \xi_{j,h}^{n+1}\|^2 \\
&= \frac{C^2}{4 C_0} \overline{\nu}_{\min}^{-1} \Delta t^2 \left\| \frac{\nabla u_j^{n+1} - \nabla u_j^n}{\Delta t} \right\|^2 + C_0 \overline{\nu}_{\min} \|\nabla \xi_{j,h}^{n+1}\|^2 \\
&= \frac{C^2}{4 C_0} \overline{\nu}_{\min}^{-1} \Delta t^2 \int_\Omega \left(\frac{1}{\Delta t} \int_{t^n}^{t^{n+1}} \nabla u_{j,t} \, dt \right)^2 d\Omega + C_0 \overline{\nu}_{\min} \|\nabla \xi_{j,h}^{n+1}\|^2 \\
&\leqslant \frac{C^2}{4 C_0} \overline{\nu}_{\min}^{-1} \Delta t \int_{t^n}^{t^{n+1}} \|\nabla u_{j,t}\|^2 \, dt + C_0 \overline{\nu}_{\min} \|\nabla \xi_{j,h}^{n+1}\|^2.
\end{aligned}
\tag{B16}
$$

For the pressure term in (B3), because $\xi_{j,h}^{n+1} \in V_h$ we have, for any $q_{j,h}^{n+1} \in Q_h$,

$$
\begin{aligned}
(p_j^{n+1}, \nabla \cdot \xi_{j,h}^{n+1}) = (p_j^{n+1} - q_{j,h}^{n+1}, \nabla \cdot \xi_{j,h}^{n+1}) &\leqslant \sqrt{d} \, \|p_j^{n+1} - q_{j,h}^{n+1}\| \|\nabla \xi_{j,h}^{n+1}\| \\
&\leqslant \frac{1}{4d \, C_0} \overline{\nu}_{\min}^{-1} \|p_j^{n+1} - q_{j,h}^{n+1}\|^2 + C_0 \, \overline{\nu}_{\min} \|\nabla \xi_{j,h}^{n+1}\|^2.
\end{aligned}
\tag{B17}
$$

The other terms are bounded as

$$\left(\frac{\eta_j^{n+1} - \eta_j^n}{\Delta t}, \xi_{j,h}^{n+1}\right) \leqslant C\left\|\frac{\eta_j^{n+1} - \eta_j^n}{\Delta t}\right\| \|\nabla \xi_{j,h}^{n+1}\| \leqslant \frac{C^2}{4C_0}\overline{\nu}_{\min}^{-1}\left\|\frac{\eta_j^{n+1} - \eta_j^n}{\Delta t}\right\|^2 + C_0\overline{\nu}_{\min}\|\nabla \xi_{j,h}^{n+1}\|^2$$

$$\leqslant \frac{C^2}{4C_0}\overline{\nu}_{\min}^{-1}\left\|\frac{1}{\Delta t}\int_{t^n}^{t^{n+1}} \eta_{j,t}\, \mathrm{d}t\right\|^2 + C_0\overline{\nu}_{\min}\|\nabla \xi_{j,h}^{n+1}\|^2$$

$$\leqslant \frac{C^2}{4C_0}\overline{\nu}_{\min}^{-1}\Delta t^{-1}\int_{t^n}^{t^{n+1}} \|\eta_{j,t}\|^2\, \mathrm{d}t + C_0\overline{\nu}_{\min}\|\nabla \xi_{j,h}^{n+1}\|^2 \tag{B18}$$

and

$$\mathrm{Intp}(u_j^{n+1}; \xi_{j,h}^{n+1}) = \left(\frac{u_j^{n+1} - u_j^n}{\Delta t} - u_{j,t}(t^{n+1}), \xi_{j,h}^{n+1}\right) \leqslant C\left\|\frac{u_j^{n+1} - u_j^n}{\Delta t} - u_{j,t}(t^{n+1})\right\| \|\nabla \xi_{j,h}^{n+1}\|$$

$$\leqslant \frac{C^2}{4C_0}\overline{\nu}_{\min}^{-1}\left\|\frac{u_j^{n+1} - u_j^n}{\Delta t} - u_{j,t}(t^{n+1})\right\|^2 + C_0\overline{\nu}_{\min}\|\nabla \xi_{j,h}^{n+1}\|^2$$

$$\leqslant \frac{C^2}{4C_0}\overline{\nu}_{\min}^{-1}\Delta t\int_{t^n}^{t^{n+1}} \|u_{j,tt}\|^2\, \mathrm{d}t + C_0\overline{\nu}_{\min}\|\nabla \xi_{j,h}^{n+1}\|^2. \tag{B19}$$

Combining (B4)–(B19), we have

$$\frac{1}{\Delta t}\left(\frac{1}{2}\|\xi_{j,h}^{n+1}\|^2 - \frac{1}{2}\|\xi_{j,h}^n\|^2 + \frac{1}{4}\|\xi_{j,h}^{n+1} - \xi_{j,h}^n\|^2\right)$$

$$+ C_0\overline{\nu}_{\min}\|\nabla \xi_{j,h}^{n+1}\|^2 + \overline{\nu}_{\min}\left(1 - 14C_0 - \frac{\|\nu_j - \overline{\nu}\|_\infty}{2\overline{\nu}_{\min}}\right)\left(\|\nabla \xi_{j,h}^{n+1}\|^2 - \|\nabla \xi_{j,h}^n\|^2\right)$$

$$+ \overline{\nu}_{\min}\left[(1-\sigma)\left(1 - 14C_0 - \frac{\|\nu_j - \overline{\nu}\|_\infty}{2\overline{\nu}_{\min}}\right) - \frac{C\Delta t}{\overline{\nu}_{\min}h}\|\nabla(u_{j,h}^n - \overline{u}_h^n)\|^2\right]\|\nabla \xi_{j,h}^n\|^2$$

$$+ \overline{\nu}_{\min}\left[\sigma\left(1 - 14C_0 - \frac{\|\nu_j - \overline{\nu}\|_\infty}{2\overline{\nu}_{\min}}\right) - \frac{\|\nu_j - \overline{\nu}\|_\infty}{2\overline{\nu}_{\min}}\right]\|\nabla \xi_{j,h}^n\|^2$$

$$\leqslant C\left[\frac{1}{\overline{\nu}_{\min}^3}\|\xi_{j,h}^n\|^2 + \Delta t\frac{\|\nu_j - \overline{\nu}\|_\infty^2}{\overline{\nu}_{\min}}\int_{t^n}^{t^{n+1}} \|\nabla u_{j,t}\|^2\mathrm{d}t \right. \tag{B20}$$

$$+ \frac{\|\nu_j - \overline{\nu}\|_\infty^2}{\overline{\nu}_{\min}}\|\nabla \eta_j^n\|^2 + \overline{\nu}_{\min}^{-1}\|\nabla(u_{j,h}^n - \overline{u}_h^n)\|^2\|\nabla \eta_j^{n+1}\|^2$$

$$+ \overline{\nu}_{\min}^{-1}\|\nabla(u_{j,h}^n - \overline{u}_h^n)\|^2\|\nabla \eta_j^n\|^2 + \overline{\nu}_{\min}^{-1}\Delta t\|\nabla(u_{j,h}^n - \overline{u}_h^n)\|^2\int_{t^n}^{t^{n+1}} \|\nabla u_{j,t}\|^2\, \mathrm{d}t$$

$$+ \overline{\nu}_{\min}^{-1}\|\nabla \eta_j^n\|^2 + \overline{\nu}_{\min}^{-1}\|\nabla u_{j,h}^n\|\|\nabla \eta_j^{n+1}\|^2 + \overline{\nu}_{\min}^{-1}\Delta t\int_{t^n}^{t^{n+1}} \|\nabla u_{j,t}\|^2\, \mathrm{d}t$$

$$+ \overline{\nu}_{\min}^{-1}\|p_j^{n+1} - q_{j,h}^{n+1}\|^2 + \overline{\nu}_{\min}^{-1}\Delta t^{-1}\int_{t^n}^{t^{n+1}} \|\eta_{j,t}\|^2\, \mathrm{d}t + \overline{\nu}_{\min}^{-1}\Delta t\int_{t^n}^{t^{n+1}} \|u_{j,tt}\|^2\mathrm{d}t\bigg].$$

Note that the generic constant C independent of Δt is used on the RHS. It, however, depends on the geometry and mesh due to the use of an inverse inequality in (B10).

Similarly to the stability analysis we take $C_0 = \frac{1}{14}(1 - \frac{\sigma+1}{2\sigma}\sqrt{\mu}) = \frac{1}{14}\frac{\varepsilon}{\sqrt{\mu}+\varepsilon}(1 - \frac{\sqrt{\mu}}{2})$ with $\sigma = \frac{\sqrt{\mu}+\varepsilon}{2-\sqrt{\mu}}$. Then (B20) becomes

$$
\begin{aligned}
&\frac{1}{\Delta t}\left(\frac{1}{2}||\xi_{j,h}^{n+1}||^2 - \frac{1}{2}||\xi_{j,h}^n||^2 + \frac{1}{4}||\xi_{j,h}^{n+1} - \xi_{j,h}^n||^2\right) \\
&\quad + \frac{1}{14}\frac{\varepsilon}{\sqrt{\mu}+\varepsilon}\left(1 - \frac{\sqrt{\mu}}{2}\right)\overline{v}_{\min}\|\nabla\xi_{j,h}^{n+1}\|^2 \\
&\quad + \overline{v}_{\min}\left[\frac{\sqrt{\mu}}{2}\frac{(2+\varepsilon)}{\sqrt{\mu}+\varepsilon} - \frac{\|v_j-\overline{v}\|_\infty}{2\overline{v}_{\min}}\right]\left(\|\nabla\xi_{j,h}^{n+1}\|^2 - \|\nabla\xi_{j,h}^n\|^2\right) \\
&\quad + \overline{v}_{\min}\left[\frac{2-2\sqrt{\mu}-\varepsilon}{2-\sqrt{\mu}}\left(\frac{\sqrt{\mu}}{2}\frac{2+\varepsilon}{\sqrt{\mu}+\varepsilon} - \frac{\|v_j-\overline{v}\|_\infty}{2\overline{v}_{\min}}\right) - \frac{C\Delta t}{\overline{v}_{\min}h}\|\nabla(u_{j,h}^n - \overline{u}_h^n)\|^2\right]\|\nabla\xi_{j,h}^n\|^2 \\
&\quad + \overline{v}_{\min}\left[\frac{\sqrt{\mu}+\varepsilon}{2-\sqrt{\mu}}\left(\frac{\sqrt{\mu}}{2}\frac{2+\varepsilon}{\sqrt{\mu}+\varepsilon} - \frac{\|v_j-\overline{v}\|_\infty}{2\overline{v}_{\min}}\right) - \frac{\|v_j-\overline{v}\|_\infty}{2\overline{v}_{\min}}\right]\|\nabla\xi_{j,h}^n\|^2 \\
&\leqslant C\left[\frac{1}{\overline{v}_{\min}^3}\|\xi_{j,h}^n\|^2 + \Delta t\frac{\|v_j-\overline{v}\|_\infty^2}{\overline{v}_{\min}}\int_{t^n}^{t^{n+1}}\|\nabla u_{j,t}\|^2\,\mathrm{d}t + \overline{v}_{\min}\|\nabla\eta_j^{n+1}\|^2\right. \\
&\quad + \frac{\|v_j-\overline{v}\|_\infty^2}{\overline{v}_{\min}}\|\nabla\eta_j^n\|^2 + \overline{v}_{\min}^{-1}\|\nabla(u_{j,h}^n - \overline{u}_h^n)\|^2\|\nabla\eta_j^{n+1}\|^2 \\
&\quad + \overline{v}_{\min}^{-1}\|\nabla(u_{j,h}^n - \overline{u}_h^n)\|^2\|\nabla\eta_j^n\|^2 + \overline{v}_{\min}^{-1}\Delta t\|\nabla(u_{j,h}^n - \overline{u}_h^n)\|^2\int_{t^n}^{t^{n+1}}\|\nabla u_{j,t}\|^2\,\mathrm{d}t \\
&\quad + \overline{v}_{\min}^{-1}\|\nabla\eta_j^n\|^2 + \overline{v}_{\min}^{-1}\|\nabla u_{j,h}^n\|\|\nabla\eta_j^{n+1}\|^2 + \overline{v}_{\min}^{-1}\Delta t\int_{t^n}^{t^{n+1}}\|\nabla u_{j,t}\|^2\,\mathrm{d}t \\
&\quad \left. + \overline{v}_{\min}^{-1}\|p_j^{n+1} - q_{j,h}^{n+1}\|^2 + \overline{v}_{\min}^{-1}\Delta t^{-1}\int_{t^n}^{t^{n+1}}\|\eta_{j,t}\|^2\,\mathrm{d}t + \overline{v}_{\min}^{-1}\Delta t\int_{t^n}^{t^{n+1}}\|u_{j,tt}\|^2\,\mathrm{d}t\right].
\end{aligned}
\tag{B21}
$$

By the convergence condition (3.3) we have

$$
\frac{\sqrt{\mu}}{2}\frac{(2+\varepsilon)}{\sqrt{\mu}+\varepsilon} - \frac{\|v_j-\overline{v}\|_\infty}{2\overline{v}_{\min}} \geqslant \frac{\sqrt{\mu}}{2}\frac{(2+\varepsilon)}{\sqrt{\mu}+\varepsilon} - \frac{\sqrt{\mu}}{2} > 0
$$

and

$$
\begin{aligned}
&\frac{\sqrt{\mu}+\varepsilon}{2-\sqrt{\mu}}\left(\frac{\sqrt{\mu}}{2}\frac{2+\varepsilon}{\sqrt{\mu}+\varepsilon} - \frac{\|v_j-\overline{v}\|_\infty}{2\overline{v}_{\min}}\right) - \frac{\|v_j-\overline{v}\|_\infty}{2\overline{v}_{\min}} \\
&\qquad \geqslant \frac{\sqrt{\mu}+\varepsilon}{2-\sqrt{\mu}}\left(\frac{\sqrt{\mu}}{2}\frac{2+\varepsilon}{\sqrt{\mu}+\varepsilon} - \frac{\sqrt{\mu}}{2}\right) - \frac{\sqrt{\mu}}{2} \\
&\qquad \geqslant \frac{\sqrt{\mu}+\varepsilon}{2-\sqrt{\mu}}\left(\frac{\sqrt{\mu}}{2}\frac{2-\sqrt{\mu}}{\sqrt{\mu}+\varepsilon}\right) - \frac{\sqrt{\mu}}{2} \geqslant \frac{\sqrt{\mu}}{2} - \frac{\sqrt{\mu}}{2} = 0
\end{aligned}
$$

and by the convergence conditions (3.2) and (3.3) we have

$$
\frac{2 - 2\sqrt{\mu} - \varepsilon}{2 - \sqrt{\mu}} \left(\frac{\sqrt{\mu}}{2} \frac{2 + \varepsilon}{\sqrt{\mu} + \varepsilon} - \frac{\|v_j - \overline{v}\|_\infty}{2\overline{v}_{\min}} \right) - \frac{C\Delta t}{\overline{v}_{\min}h} \|\nabla(u_{j,h}^n - \overline{u}_h^n)\|^2
$$

$$
\geqslant \frac{2 - 2\sqrt{\mu} - \varepsilon}{2 - \sqrt{\mu}} \left(\frac{\sqrt{\mu}}{2} \frac{2 - \sqrt{\mu}}{\sqrt{\mu} + \varepsilon} \right) - \frac{(2 - 2\sqrt{\mu} - \varepsilon)\sqrt{\mu}}{2(\sqrt{\mu} + \varepsilon)}
$$

$$
\geqslant \frac{(2 - 2\sqrt{\mu} - \varepsilon)\sqrt{\mu}}{2(\sqrt{\mu} + \varepsilon)} - \frac{(2 - 2\sqrt{\mu} - \varepsilon)\sqrt{\mu}}{2(\sqrt{\mu} + \varepsilon)} \geq 0.
$$

Summing (B20) from $n = 1$ to $N - 1$ and multiplying both sides by Δt gives

$$
\frac{1}{2}\|\xi_{j,h}^N\|^2 + \frac{1}{4} \sum_{n=0}^{N-1} \|\xi_{j,h}^{n+1} - \xi_{j,h}^n\|^2
$$

$$
+ \frac{1}{14} \frac{\varepsilon}{\sqrt{\mu} + \varepsilon} \left(1 - \frac{\sqrt{\mu}}{2} \right) \overline{v}_{\min} \Delta t \sum_{n=0}^{N-1} \|\nabla \xi_{j,h}^{n+1}\|^2
$$

$$
+ \overline{v}_{\min} \Delta t \left[\frac{\sqrt{\mu}}{2} \frac{(2 + \varepsilon)}{\sqrt{\mu} + \varepsilon} - \frac{\|v_j - \overline{v}\|_\infty}{2\overline{v}_{\min}} \right] \|\nabla \xi_{j,h}^N\|^2
$$

$$
\leqslant \frac{1}{2}\|\xi_{j,h}^0\|^2 + \overline{v}_{\min} \Delta t \left[\frac{\sqrt{\mu}}{2} \frac{(2 + \varepsilon)}{\sqrt{\mu} + \varepsilon} - \frac{\|v_j - \overline{v}\|_\infty}{2\overline{v}_{\min}} \right] \|\nabla \xi_{j,h}^0\|^2 + \frac{C\Delta t}{\overline{v}_{\min}^3} \sum_{n=0}^{N-1} \|\xi_{j,h}^n\|^2
$$

$$
+ C\Delta t \sum_{n=0}^{N-1} \left[\Delta t \frac{\|v_j - \overline{v}\|_\infty^2}{\overline{v}_{\min}} \int_{t^n}^{t^{n+1}} \|\nabla u_{j,t}\|^2 \, dt + \overline{v}_{\min} \|\nabla \eta_j^{n+1}\|^2 \right.
$$

$$
+ \frac{\|v_j - \overline{v}\|_\infty^2}{\overline{v}_{\min}} \|\nabla \eta_j^n\|^2 + \overline{v}_{\min}^{-1} \|\nabla(u_{j,h}^n - \overline{u}_h^n)\|^2 \|\nabla \eta_j^{n+1}\|^2
$$

$$
+ \overline{v}_{\min}^{-1} \|\nabla(u_{j,h}^n - \overline{u}_h^n)\|^2 \|\nabla \eta_j^n\|^2 + \overline{v}_{\min}^{-1} \Delta t \|\nabla(u_{j,h}^n - \overline{u}_h^n)\|^2 \int_{t^n}^{t^{n+1}} \|\nabla u_{j,t}\|^2 \, dt
$$

$$
+ \overline{v}_{\min}^{-1} \|\nabla \eta_j^n\|^2 + \overline{v}_{\min}^{-1} \Delta t \int_{t^n}^{t^{n+1}} \|\nabla u_{j,t}\|^2 \, dt + \overline{v}_{\min}^{-1} \|\nabla \eta_j^{n+1}\|^2 \|\nabla u_{j,h}^n\|
$$

$$
+ \overline{v}_{\min}^{-1} \|p_j^{n+1} - q_{j,h}^{n+1}\|^2 + \overline{v}_{\min}^{-1} \Delta t^{-1} \int_{t^n}^{t^{n+1}} \|\eta_{j,t}\|^2 \, dt + \overline{v}_{\min}^{-1} \Delta t \int_{t^n}^{t^{n+1}} \|u_{j,tt}\|^2 \, dt \right].
$$

Using the Ritz projection error (B2) and the result (2.4) from the stability analysis, i.e., $\Delta t \sum_{n=0}^{N-1} \|\nabla u_{j,h}^n\|^2 \leqslant C$, we have

$$
C\overline{v}_{\min}^{-1} \Delta t \sum_{n=0}^{N-1} \|\nabla \eta_j^{n+1}\|^2 \|\nabla u_{j,h}^n\| \leqslant C\overline{v}_{\min}^{-1} h^{2k} \Delta t \sum_{n=0}^{N-1} \|u_j^{n+1}\|_{k+1}^2 \|^2 \|\nabla u_{j,h}^n\| \tag{B22}
$$

$$\leqslant C\overline{v}_{\min}^{-1}h^{2k}\left(\Delta t\sum_{n=0}^{N-1}\|u_j^{n+1}\|_{k+1}^4+\Delta t\sum_{n=0}^{N-1}\|\nabla u_{j,h}^n\|^2\right)\tag{B23}$$

$$\leqslant C\overline{v}_{\min}^{-1}h^{2k}\|\|u_j\|\|_{4,k+1}^4+C\overline{v}_{\min}^{-1}h^{2k}.$$

By applying again the Ritz projection error (B2) and the interpolation error (1.6) we have

$$\frac{1}{2}\|\xi_{j,h}^N\|^2+\overline{v}_{\min}\Delta t\left[\frac{\sqrt{\mu}}{2}\frac{(2+\varepsilon)}{\sqrt{\mu}+\varepsilon}-\frac{\|v_j-\overline{v}_{\min}\|_\infty}{2\overline{v}_{\min}}\right]\|\nabla\xi_{j,h}^N\|^2+\sum_{n=0}^{N-1}\frac{1}{4}\|\xi_{j,h}^{n+1}-\xi_{j,h}^n\|^2$$

$$+\frac{1}{15}\frac{\varepsilon}{\sqrt{\mu}+\varepsilon}\left(1-\frac{\sqrt{\mu}}{2}\right)\overline{v}_{\min}\Delta t\sum_{n=0}^{N-1}\|\nabla\xi_{j,h}^{n+1}\|^2$$

$$\leqslant\frac{1}{2}\|\xi_{j,h}^0\|^2+\overline{v}_{\min}\Delta t\left[\frac{\sqrt{\mu}}{2}\frac{(2+\varepsilon)}{\sqrt{\mu}+\varepsilon}-\frac{\|v_j-\overline{v}\|_\infty}{2\overline{v}_{\min}}\right]\|\nabla\xi_{j,h}^0\|^2+\frac{C\Delta t}{\overline{v}_{\min}^3}\sum_{n=0}^{N-1}\|\xi_{j,h}^n\|^2\tag{B24}$$

$$+C\Delta t^2\frac{\|v_j-\overline{v}\|_\infty^2}{\overline{v}_{\min}}\|\nabla u_{j,t}\|_{2,0}^2+C\overline{v}_{\min}h^{2k}\|\|u_j\|\|_{2,k+1}^2+C\frac{\|v_j-\overline{v}\|_\infty^2}{\overline{v}_{\min}}h^{2k}\|\|u_j\|\|_{2,k+1}^2$$

$$+Ch^{2k+1}\Delta t^{-1}\|\|u_j\|\|_{2,k+1}^2+Ch\Delta t\|\nabla u_{j,t}\|_{2,0}^2+C\overline{v}_{\min}^{-1}h^{2k}\|\|u_j\|\|_{2,k+1}^2$$

$$+C\overline{v}_{\min}^{-1}\Delta t^2\|\nabla u_{j,t}\|_{2,0}^2+C\overline{v}_{\min}^{-1}h^{2k}\|\|u_j\|\|_{4,k+1}^4+C\overline{v}_{\min}^{-1}h^{2k}$$

$$+C\overline{v}_{\min}^{-1}h^{2s+2}\|\|p_j\|\|_{2,s+1}^2+C\overline{v}_{\min}^{-1}h^{2k+2}\|u_{j,t}\|_{2,k+1}^2+C\overline{v}_{\min}^{-1}\Delta t^2\|u_{j,tt}\|_{2,0}^2.$$

The next step is the application of the discrete Gronwall inequality (see Girault & Raviart, 1979, p. 176):

$$\frac{1}{2}\|\xi_{j,h}^N\|^2+\overline{v}_{\min}\Delta t\left(\frac{\sqrt{\mu}}{2}\frac{(2+\varepsilon)}{\sqrt{\mu}+\varepsilon}-\frac{\|v_j-\overline{v}\|_\infty}{2\overline{v}_{\min}}\right)\|\nabla\xi_{j,h}^N\|^2+\sum_{n=0}^{N-1}\frac{1}{4}\|\xi_{j,h}^{n+1}-\xi_{j,h}^n\|^2$$

$$+\frac{1}{14}\frac{\varepsilon}{\sqrt{\mu}+\varepsilon}\left(1-\frac{\sqrt{\mu}}{2}\right)\overline{v}_{\min}\Delta t\sum_{n=0}^{N-1}\|\nabla\xi_{j,h}^{n+1}\|^2\tag{B25}$$

$$\leqslant e^{\frac{CT}{\overline{v}_{\min}^3}}\left\{\frac{1}{2}\|\xi_{j,h}^0\|^2+\overline{v}_{\min}\Delta t\left[\frac{\sqrt{\mu}}{2}\frac{(2+\varepsilon)}{\sqrt{\mu}+\varepsilon}-\frac{\|v_j-\overline{v}\|_\infty}{2\overline{v}_{\min}}\right]\|\nabla\xi_{j,h}^0\|^2\right.$$

$$+C\left[\Delta t^2\frac{\|v_j-\overline{v}\|_\infty^2}{\overline{v}_{\min}}\|\|\nabla u_{j,t}\|\|_{2,0}^2+\overline{v}_{\min}h^{2k}\|\|u_j\|\|_{2,k+1}^2+\frac{\|v_j-\overline{v}\|_\infty^2}{\overline{v}_{\min}}h^{2k}\|\|u_j\|\|_{2,k+1}^2\right.$$

$$+h^{2k+1}\Delta t^{-1}\|\|u_j\|\|_{2,k+1}^2+Ch\Delta t\|\|\nabla u_{j,t}\|\|_{2,0}^2+\overline{v}_{\min}^{-1}h^{2k}\|\|u_j\|\|_{2,k+1}^2$$

$$+\overline{v}_{\min}^{-1}\Delta t^2\|\|\nabla u_{j,t}\|\|_{2,0}^2+\overline{v}_{\min}^{-1}h^{2k}\|\|u_j\|\|_{4,k+1}^4+\overline{v}_{\min}^{-1}h^{2k}$$

$$\left.\left.+\overline{v}_{\min}^{-1}h^{2s+2}\|\|p_j\|\|_{2,s+1}^2+\overline{v}_{\min}^{-1}h^{2k+2}\|\|u_{j,t}\|\|_{2,k+1}^2+\overline{v}_{\min}^{-1}\Delta t^2\|\|u_{j,tt}\|\|_{2,0}^2\right]\right\}.$$

Recall that $e_j^n = \eta_j^n + \xi_{j,h}^n$. Using the triangle inequality on the error equation to split the error terms into terms of η_j^n and $\xi_{j,h}^n$ gives

$$\frac{1}{2}\|e_j^N\|^2 + \frac{1}{14}\frac{\varepsilon}{\sqrt{\mu}+\varepsilon}\left(1 - \frac{\sqrt{\mu}}{2}\right)\overline{v}_{\min}\Delta t\sum_{n=0}^{N-1}\|\nabla e_j^{n+1}\|^2$$

$$\leqslant \frac{1}{2}\|\xi_{j,h}^N\|^2 + \frac{1}{14}\frac{\varepsilon}{\sqrt{\mu}+\varepsilon}\left(1 - \frac{\sqrt{\mu}}{2}\right)\overline{v}_{\min}\Delta t\sum_{n=0}^{N-1}\|\nabla \xi_{j,h}^{n+1}\|^2$$

$$+ \frac{1}{2}\|\eta_j^N\|^2 + \frac{1}{14}\frac{\varepsilon}{\sqrt{\mu}+\varepsilon}\left(1 - \frac{\sqrt{\mu}}{2}\right)\overline{v}_{\min}\Delta t\sum_{n=0}^{N-1}\|\nabla \eta_j^{n+1}\|^2$$

and

$$\frac{1}{2}\|\xi_{j,h}^0\|^2 + \left[\frac{\sqrt{\mu}}{2}\frac{(2+\varepsilon)}{\sqrt{\mu}+\varepsilon} - \frac{\|v_j - \overline{v}\|_\infty}{2\overline{v}_{\min}}\right]\overline{v}_{\min}\Delta t\|\nabla \xi_{j,h}^0\|^2$$

$$\leqslant \frac{1}{2}\|e_j^0\|^2 + \left[\frac{\sqrt{\mu}}{2}\frac{(2+\varepsilon)}{\sqrt{\mu}+\varepsilon} - \frac{v_j - \overline{v}\|_\infty}{2\overline{v}_{\min}}\right]\overline{v}_{\min}\Delta t\|\nabla e_j^0\|^2$$

$$+ \frac{1}{2}\|\eta_j^0\|^2 + \left[\frac{\sqrt{\mu}}{2}\frac{(2+\varepsilon)}{\sqrt{\mu}+\varepsilon} - \frac{v_j - \overline{v}\|_\infty}{2\overline{v}_{\min}}\right]\overline{v}_{\min}\Delta t\|\nabla \eta_j^0\|^2.$$

Applying inequality (B25), using the previous bounds for η_j^n terms, and absorbing constants into a new constant C, completes the proof of Theorem 3.1.